ISRN LUTFD2/TFRT-5646-SE

Safe Manual Control of Unstable Systems

Johan Åkesson

Department of Automatic Control
Lund Institute of Technology
September 2000

Contents

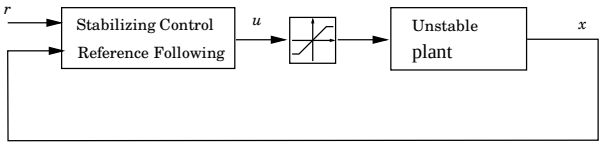

Figure 1 An illustration of the problem formulation dealt with in this work.

1. Introduction

This report deals with manual control of an unstable system with actuator saturation. The control task is critical, manual control must not be performed in such way that it causes instability. Typically this problem arises when the plant has limitations on the control signal, i.e saturation and/or rate limits. The available control authority is thus limited and must be shared between stabilization and manual control. (See for example Åström and Brufani (1997) and Brufani (1997)).

Examples of manual control of unstable systems in practice are modern fighter aircrafts, e.g JAS 39 Gripen. The aircraft is unstable in some flight conditions, and has to be stabilized by the control system in order to operate. The problem here is the rate limited actuators, that may reduce the stability drastically when saturated. This issue is discussed further in Rundqwist *et al.* (1997).

Interesting points concerning control of unstable systems are made in Stein (1990). In this lecture, the importance of the safety aspect of control systems is discussed.

1.1 Problem Formulation

The problem formulation can be illustrated as in fig 1. The plant to be controlled is unstable, and the control signal is restricted by saturation. There are two objectives, possibly conflicting, for the controller. The first and most important is to guarantee stability of the closed loop system. This should always be given the highest priority. The second objective is to perform manual control of a certain state of the process, e.g. position or velocity. This introduction of reference signal may lead to violation of the stabilization condition if the authority of this control task is not limited. Strategies to achieve “good” reference following (the meaning of “good” is discussed in Section 4.1) with guaranteed stability is thus the main subject of this work.

1.2 Experiments

Practical experiments have been an important part of this work. For this purpose we have used an inverted pendulum of the Furuta type. In this version, the pendulum is attached to a rotating arm instead of the classic linear cart, see fig 4. This is a nice property since there exists no end points restricting the pivot point of the pendulum. Both position control and velocity control of the pivot point may thus be performed without considerations about the cart track ending. The inverted pendulum may seem very different from a complex fighter aircraft, but they share one important characteristic feature; both are unstable. Thus, the inverted pendulum

serves as a suitable plant for our purposes.

The control task we have chosen, was to control the velocity of the pivot point of the pendulum, subject to a stability constraint. As for the stability constraint, we have considered it a failure if the pendulum passes its horizontal position. As discussed earlier, the problem is that the control authority is limited, i.e there is a saturation on the plant input. In order to guarantee sufficient authority to the stabilizing control, restrictions have to be imposed on the reference signal.

1.3 Road map

We will start in Section 2 by giving a simple example that clearly demonstrates the problem formulation. A detailed description of the inverted pendulum is given in Section 3. A stabilizing control law is derived. This section also discusses the issues of swing up of the pendulum and friction compensation. This sections are less relevant for the solution of the manual control problem and may be skipped, but they are indeed recommended for the interested reader.

In Section 4 a framework for manual control is developed. Fundamental control performance limitations are discussed, as well as different servo mechanisms. Section 5 deals with the actual problem of saturating control inputs. Different theoretical approaches to the problem are considered, including a simple heuristic method, admissible set theory and a controller based upon a phase plane analysis of the linearized system. In Section 6, experiments on a real pendulum are discussed, where some of the strategies described in Section 5 was implemented. Results and conclusions are summarized in Section 7, and finally, in Section 8 the experimental set up is described.

1.4 Results

This work deals with both practical and theoretical aspects of the problem defined above. The theoretical results are indeed promising. They involve for instance a review of the reference governor and a derivation of a controller based on cascaded saturations. Both designs performed very well in simulations.

However, despite the theoretical design achievements, control of the real Furuta pendulum proved hard. The controllers had to be carefully tuned in order to work. But although troublesome, the implementation of the controllers did solve the stabilization problem also for the real pendulum.

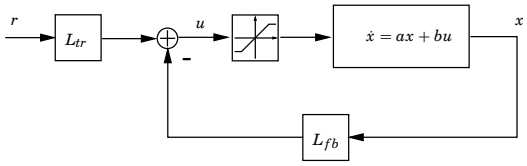

Figure 2 A first order system with a saturation on the input.

2. A Motivational Example

To illustrate the problem of controlling unstable plants with limited control authority (in our case saturation) we will give a simple example. Consider the controlled first order system in figure 2. The interesting case is when $a > 0$, i.e the system is unstable, in which case the saturation makes the stabilizing control task critical. The stability of a linear system is determined only by its closed loop properties, whereas for nonlinear systems the initial conditions (or input signal) also has to be considered. Let us take a brief look at the conditions for stabilizability of the system in terms of admissible values of the state x.

Let the control law be

$$u = L_{fb}x + L_{tr}r$$

where L_{fb} is used to stabilize the system and L_{tr} is tuned to give unit steady state gain. Under these circumstances we could calculate the values of the state x, for which the system is recoverable. We do the calculations in steady state ($\dot{x} = 0$) for simplicity.

Now, if we let the saturation limits be $\pm u_{sat}$ yielding

$$|u| < u_{sat}.$$

This gives us the condition

$$|x| < \frac{bu_{sat}}{a}$$

as for admissible state values. Since the steady state gain is 1, this implies that these are the limits for admissible reference values as well. The controller analyzed here, leaves it to the user to make sure no destabilizing inputs are applied to the system, which is of course not desirable. Methods for solving this problem are discussed in, for example, Patcher and Miller (1998).

The effect of the input saturation can be seen in figure 3. Although this example is simple, it shows that the combination of unstable systems and limited control authority is a critical problem.

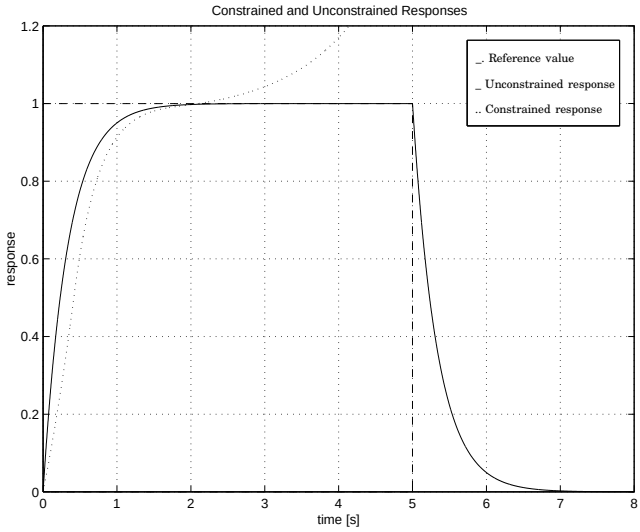

Figure 3 The effect of saturated input. In the unconstrained case, there is no saturation at all on the input. In the constrained case, the reference value is set slightly higher than the limit calculated above.

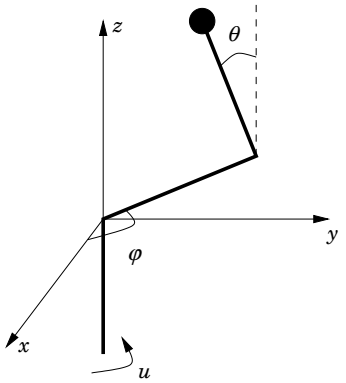

Figure 4 A schematic picture of the Furuta pendulum

3. The Furuta Pendulum

In this section a mathematical model for the Furuta pendulum which was used in the experiments is presented. The model is based on the derivation in Gäfvert (1998), only the results are given here.

Consider the Furuta pendulum in fig 4. Let the length of the pendulum be l, the mass of the weight M, the mass of the pendulum m, its moment of inertia J and the moment of inertia for the arm J_p. The length of the arm is r. The angle of the pendulum, θ, is defined to be zero when in upright position and positive when the pendulum is moving clockwise. The angle of the arm, φ is positive when the arm is moving in counter clockwise direction. Further, the central vertical axis is connected to a DC motor which adds a torque proportional to the control signal u.

3.1 Mathematical model

The complete derivation of the Furuta pendulum dynamics is excluded here. The derivation is based on Lagrange theory and can be read in Gäfvert (1998).

Using the definitions made above, the equations of motion can be written

$$\begin{aligned}(J_p + Ml^2)(\ddot{\theta} - \dot{\varphi}^2 \sin\theta\cos\theta) + Mrl\ddot{\varphi}\cos\theta - gl(M + m/2)\sin\theta = 0 \\ Mrl\ddot{\theta}\cos\theta - Mrl\dot{\theta}^2\sin\theta + 2(J_p + ml^2)\dot{\theta}\dot{\varphi}\sin\theta\cos\theta \\ +(J + mr^2 + Mr^2 + (J_p + ml^2)\sin^2\theta)\ddot{\varphi} = u.\end{aligned} \tag{1}$$

Introduce

$$\begin{aligned} a &= J_p + Ml^2 & b &= J + Mr^2 + mr^2 \\ c &= Mrl & d &= lg(M + m/2)\end{aligned}$$

and the equations of motion can be rewritten:

$$\begin{aligned} a\ddot{\theta} - a\dot{\varphi}^2\sin\theta\cos\theta + c\ddot{\varphi}\cos\theta - d\sin\theta = 0 \\ c\ddot{\theta}\cos\theta - c\dot{\theta}^2\sin\theta + 2a\dot{\theta}\dot{\varphi}\sin\theta\cos\theta + (b + a\sin^2\theta)\ddot{\varphi} = u.\end{aligned} \tag{2}$$

The coefficients for the pendulum used in the experiments are (see Svensson (1998)):

$$\begin{aligned} l &= 0.413\ m & r &= 0.235\ m \\ M &= 0.01\ kg & J &= 0.05\ kgm^2 \\ J_p &= 0.0009\ kgm^2 & m &= 0.02\ kg\end{aligned}$$

This model was used for further calculations and simulation.

3.2 Stabilization of the pendulum

Our first objective before manual control can be performed is to stabilize the pendulum in upright position. Notice, that the angular velocity of the arm is taken into account when the linearization is made. This is because our objective is to perform velocity control, and gain scheduling will be used to modify the control law with varying velocity. This means that the controller will not be linear, it will change with varying arm velocity.

Since all states is measurable, linear state feedback is used. The method is simple and allow arbitrary placement of the closed loop poles. It is then necessary to derive a linear model of the pendulum. Introduce the state vector

$$x = \begin{pmatrix} \theta & \dot{\theta} & \varphi & \dot{\varphi} \end{pmatrix}^T$$

and linearization of the system (2) around

$$x = \begin{pmatrix} 0 & 0 & 0 & \dot{\varphi}_0 \end{pmatrix}^T$$

gives

$$\dot{x} = Ax + Bu = \begin{pmatrix} 0 & 1 & 0 & 0 \\ \frac{ab\dot{\varphi}_0^2 + bd}{ab-c^2} & 0 & 0 & 0 \\ 0 & 0 & 0 & 1 \\ \frac{-ac\dot{\varphi}_0^2 - cd}{ab-c^2} & 0 & 0 & 0 \end{pmatrix} x + \begin{pmatrix} 0 \\ \frac{-c}{ab-c^2} \\ 0 \\ \frac{a}{ab-c^2} \end{pmatrix} u. \tag{3}$$

In the following, we will use

$$\alpha = \frac{ab\dot{\varphi}_0^2 + bd}{ab - c^2} \quad \beta = \frac{-c}{ab - c^2}$$
$$\gamma = \frac{-ac\dot{\varphi}_0^2 - cd}{ab - c^2} \quad \varepsilon = \frac{a}{ab - c^2}$$

yielding the state space description

$$\dot{x} = \begin{pmatrix} 0 & 1 & 0 & 0 \\ \alpha & 0 & 0 & 0 \\ 0 & 0 & 0 & 0 \\ \gamma & 0 & 0 & 0 \end{pmatrix} x + \begin{pmatrix} 0 \\ \beta \\ 0 \\ \varepsilon \end{pmatrix} u \tag{4}$$

$$= \begin{pmatrix} 0 & 1 & 0 & 0 \\ 31.32 & 0 & 0 & 0 \\ 0 & 0 & 0 & 1 \\ -0.5584 & 0 & 0 & 0 \end{pmatrix} x + \begin{pmatrix} 0 \\ -71.23 \\ 0 \\ 191.2 \end{pmatrix} u. \tag{5}$$

The control law can be written

$$u = -Lx \tag{6}$$

where

$$L = \begin{pmatrix} l_1 & l_2 & l_3 & l_4 \end{pmatrix}.$$

The control law (6) applied on the system (3) gives the closed loop dynamics

$$\dot{x} = (A - BL)x.$$

The feedback vector L may be obtained in several ways, we choose to use LQ optimal control. This method has good intuitive interpretations, and is well suited for this purpose. For a brief summary of the LQ design technique, see A.

The design parameters available to us when using LQ design are the weighting matrices Q and R. Q is used to allocate penalty weights to the states, where as R is used to penalize the control signal. When stabilizing the pendulum, our objective is to make θ and φ close to zero (indicating large weights) while we care less about the velocities $\dot{\theta}$ and $\dot{\varphi}$ (smaller

penalties). The control signal weight will be used to tune the feedback gain for good performance.

Since we would like to keep all states close to zero the controller is calculated using the linearized model with $\dot{\varphi}_0 = 0$.

The design matrices used for the experiments were:

$$\begin{aligned} Q &= \begin{pmatrix} 100 & 0 & 0 & 0 \\ 0 & 1 & 0 & 0 \\ 0 & 0 & 11 & 0 \\ 0 & 0 & 0 & 0.25 \end{pmatrix} \\ R &= 80. \end{aligned}$$

This design gives the state feedback vector

$$L = \begin{pmatrix} -5.703 & -1.009 & -0.3708 & -0.2233 \end{pmatrix}.$$

3.3 Swing Up

An issue that has not so much to do with the main problem of manual control is swinging up the pendulum from rest to upright position. Never the less it is a practical feature to implement, and a nice feature for a demonstration. A brief description f a swing up strategy will be presented, interested readers are encouraged to consult Åström and Furuta (1999)

In this section a simplified model of the pendulum will be used. Instead of the Furuta pendulum a pendulum attached to a linear cart is modeled. The reason for this is that the calculations will be significantly easier and the model will still be sufficiently accurate for our purposes. Using the same terminology as above, the equations of motion may be written

$$\begin{aligned} J_p \frac{d^2\theta}{dt} &= Mgl \sin\theta - Mla \cos\theta \\ \frac{d^2\varphi}{dt^2} &= a \end{aligned} \tag{7}$$

where a is the applied acceleration.

Introducing the normalizations

$$\omega_0 = \sqrt{\frac{Mgl}{J_p}} \quad u = \frac{a}{g}$$

the equations of motion may be rewritten as

$$\begin{aligned} \frac{d^2\theta}{dt} &= \omega_0^2 \sin\theta - \omega_0^2 u \cos\theta \\ \frac{d^2\varphi}{dt} &= ug \end{aligned}$$

Swing Up by Energy Control The strategy used is based on energy control and is presented in Åström and Furuta (1999). The basic idea is to pump energy into the system, so that it finally contains enough energy to pass the upright equilibrium. Well there, switching to a control law that catches and stabilizes the pendulum is performed.

The energy of the uncontrolled pendulum, using the same terminology as above, may be expressed as

$$E_n = \frac{E}{Mgl} = \frac{\dot{\theta}^2}{2\omega_0^2} + \cos\theta - 1.$$

The energy is thus zero when the pendulum is at rest in upright position. The energy is normalized with respect to Mgl.

A control law proposed in Åström and Furuta (1999) is

$$u = sat(k(E_n - E_0)sign(\dot{\theta}\cos\theta)).$$

E_0 is here the desired energy of the system, i.e zero. The design parameters for this method is k and the saturation limits. In our implementation k was set to 100 and the saturation limits to ± 1. This control law performs the desired swing up.

The control law presented above perform a swing up that makes the pendulum pass the upright equilibrium. However, it remains to catch and stabilize the pendulum. This is done by switching from the swing up control law to a catch control law and finally to a stabilizing control law. LQ theory is used for calculation of the catching controller. Large punishments on the states θ and $\dot{\theta}$ and a smaller punishment on $\dot{\varphi}$ gives a LQ controller with the desired properties. When the pendulum is caught, switching to the stabilizing controller is performed.

A Nonlinear Observer In order to implement the swing up strategy measures of θ and $\dot{\theta}$ is needed. This is a problem since both this signals are discontinues at a certain angle. The measurement of θ exhibits a step form 0 to 2π at this angle, which can be dealt with by adding an offset to the measured signal. $\dot{\theta}$ however exhibits more serious discontinuities and we have therefor chosen to use a nonlinear observer presented in Eker and Åström (1996) in order to obtain an estimate of $\dot{\theta}$.

The nonlinear observer has the following structure:

$$\begin{aligned}\frac{d\hat{x}_1}{dt} &= \hat{x}_2 + k_1(x_1 - \hat{x}_1)\\ \frac{d\hat{x}_2}{dt} &= \omega_0^2 \sin\hat{x}_1 + \omega_0^2 u\cos\hat{x}_1 + k_2(x_1 - \hat{x}_1)\end{aligned}$$

where $x_1 = \theta$ and $x_2 = \dot{\theta}$. The design parameters k_1 and k_2 were set to 20 and 60 respectively. The nonlinear observer produced a sufficiently accurate estimate in order to perform successful swing up of the pendulum. (Notice that the measure of θ was used directly for the swing up control law, not the estimate.)

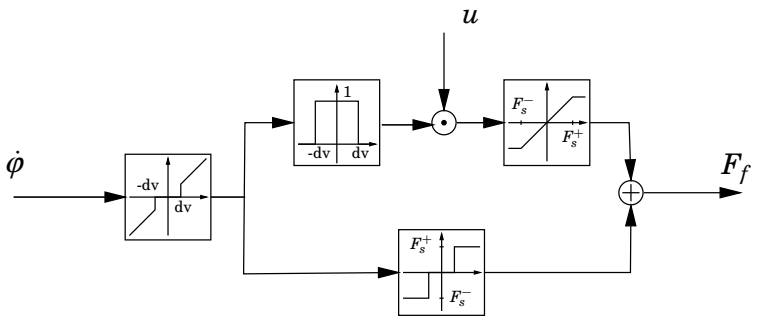

Figure 5 A schematic figure of the Karnopp friction model.

3.4 Friction

On the process used for the experiments friction is a severe complication that can not be neglected. Notice however that it is the friction in the arm (and motor) that is severe, friction in the pendulum pivot point is neglected. The friction gives rise to limit cycles, see Svensson (1998). Friction compensation is therefor highly desirable. We have chosen to use a simple model, Coulomb friction with stiction, which can be written

$$F_f(\dot{\varphi},u) = \begin{cases} F_c^+ & \dot{\varphi} > 0 \\ F_s^+ & \dot{\varphi} = 0, \quad u > F_c^+ \\ u & \dot{\varphi} = 0, \quad F_s^- < u < F_s^+ \\ F_s^- & \dot{\varphi} = 0, \quad u < F_s^- \\ F_c^- & \dot{\varphi} < 0 \end{cases}$$

The dimension of the friction is angular acceleration, which gives convenient integration with the process model. In the implementation used in the experiments the friction model is simplified further by

$$\begin{aligned} F_s^+ &= F_c^+ \\ F_s^- &= F_c^- \end{aligned}$$

Friction compensation is then performed by modifying the control law (6):

$$u = Lx + F_f.$$

In order to perform the friction compensation, the values of F_c^+ and F_c^- have to be estimated. Throughout the experiments we made, this proved to be a problem. The friction on the real process changes with a number of different parameters, temperature and wear being only two examples. The friction parameters were re-estimated several times during the experiments.

To perform the estimation we used a simple technique, where the arm velocity of the pendulum $\dot{\varphi}$ were controlled by a PI controller. The pendulum itself was allowed to be at rest in its downward position. Since the controlled entity then may be modeled as an integrator, the only control action needed (when the desired velocity is reached) is to overcome the friction. From this simple experiment we obtained (crude) measures of the values

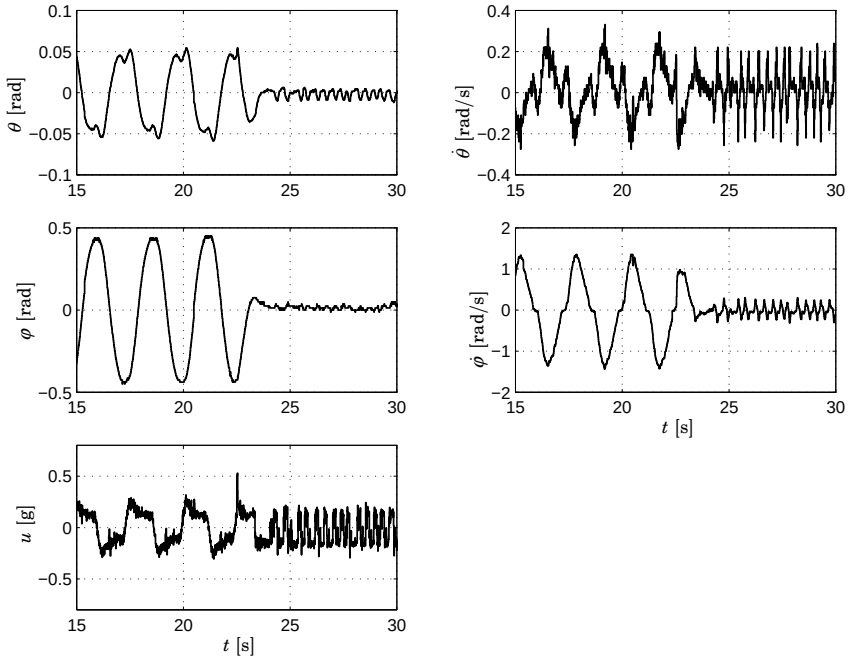

Figure 6 The effect of friction compensation. Notice the significant reduction of the amplitude of the limit cycle for the arm angle. Initially, there is now friction compensation. Friction compensation is activated at $t = 23\ s$.

F_c^+ and F_c^-. One observation we made was that the estimated friction was asymmetric, see further Canudas de Vit *et al.* (1987).

A practical problem when dealing with the real process is that the measured velocity of the arm is not zero when the arm is at rest, there is a small bias and also measurement noise. To deal with this the Karnopp model presented in Olsson (1996), p. 29 is used. A schematic figure of the model is shown in fig 5. The arm velocity is set to zero if it is within the tolerance limits $\pm$dv. In this case compensation for the stiction effect is performed, otherwise friction compensation corresponding to Coulomb friction is used.

The effect of the friction compensation is significant, the limit cycle is not entirely eliminated, but reduced in amplitude (see fig 6).

4. A Framework for Manual Control

In this section we shall establish the framework needed to analyze the saturation problem, which will be done in the next section. First, we define the objectives for the control system, and discuss what is meant by "good control". A new, reduced state space model needed for the controller is derived. An important issue is what control performance to expect from the closed loop system, given the nature of the plant. An analysis of such limitations will also be given in this section. Finally common controller structures for servo mechanisms will be discussed.

4.1 Objectives

Before investigating the different methods further the objectives of the control system and a few measures for evaluation should be discussed. The meaning of "good control" depends on the process and the demands on the closed loop system. Here we choose to consider two measures of control performance; rise times and state deviations. This choice reflects our ultimate objective, that is, fast and accurate tracking.

The rise time for a step is a measure of how fast and well damped the response is. A fast and reasonably well damped response is of course desired. The settling time is here defined as the time from the reference step to the time from which the response stays within given deviations (*e.g.* $\pm$ 10%) from the reference.

As a measure of the state deviations it is natural to use the cost function given in the LQ problem (see also appendixA):

$$J = \int_0^\infty \left(x^T Q x + u^T R u \right) dt$$

This quadratic cost measure is determined by the matrices Q and R, which may or may not be the same as those used in the controller design. If there is a physical meaning of state deviations and control energy cost, these cost matrices might be used for control performance evaluation although different from those used in the control design. In our case the controller design Q and R were selected through an iterative process to achieve reasonable responses, and not by considering the cost of state deviations or control energy. For the cost measure, Q and R were chosen as:

$$\begin{aligned} Q &= \begin{pmatrix} 10 & 0 & 0 \\ 0 & 1 & 0 \\ 0 & 0 & 0.3 \end{pmatrix} \\ R &= 8. \end{aligned}$$

This choice mostly penalizes the tracking state, $\dot{\varphi}$, but some credit are given to controllers that use little control energy.

4.2 Velocity Control

When velocity control of the pivot point is performed, it is not a good choice to use the measure of the state φ for feedback. Only θ, $\dot{\theta}$ and $\dot{\varphi}$ should be

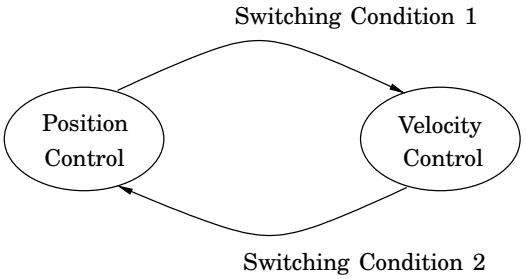

Figure 7 A finite state machine for switching between stabilization and velocity control.

used by the state feedback control law. Notice that it would not be acceptable to set the l_3 element in the control law (6) to zero, since this would yield a different controller that would not be optimal. We solve this by deriving a new control law based on a reduced state space model containing only the states θ, $\dot{\theta}$ and φ.

Use of this reduced control law may result in the pivot point drifting even when the velocity reference is set to zero. To avoid this, switching between the stabilizing control law derived in Section 3.2 and the specialized velocity control law is performed. This switching strategy may be described by a finite state machine, see Figure 7. The switching conditions are

- *Switching condition 1*: The reference signal deviates from zero.
- *Switching condition 2*: Both the velocity reference and the velocity of the pivot point have been zero for 1 s.

If the new state space vector

$$\bar{x} = \begin{pmatrix} \theta & \dot{\theta} & \dot{\varphi} \end{pmatrix}^T$$

is introduced the, system (3) may be rewritten as

$$\begin{aligned} \dot{\bar{x}} = \bar{A}\bar{x} + \bar{B}u &= \begin{pmatrix} 0 & 1 & 0 \\ \alpha & 0 & 0 \\ \gamma & 0 & 0 \end{pmatrix} \bar{x} + \begin{pmatrix} 0 \\ \beta \\ \varepsilon \end{pmatrix} u \\ &= \begin{pmatrix} 0 & 1 & 0 \\ 31.32 & 0 & 0 \\ -0.5584 & 0 & 0 \end{pmatrix} \bar{x} + \begin{pmatrix} 0 \\ -71.23 \\ 191.2 \end{pmatrix} u \end{aligned} \tag{8}$$

Applying the control law

$$u = \bar{L}(r - \bar{x}) \tag{9}$$

where r is the reference signal to be tracked. r is actually a vector; $r = (0 \; 0 \; \dot{\varphi}_r)$, where the two zeros indicate the desired values of the states θ and $\dot{\theta}$. (This way of introducing reference values into the state feedback loop will be discussed and further developed in the sections below.)

4.3 Fundamental Performance Limitations

The state feedback controller may be calculated in several ways, striving to achieve good tracking performance. But before calculating any controller at all, we should consider what performance we could expect from the (linear) closed loop system. At this stage we are only considering limitations imposed by the linearized model of the plant, and not restrictions deriving from the limited control authority discussed above.

In Åström (1999), methods for determining achievable performance, given the nature of the plant. Performance is measured as the closed loop bandwidth, ω_{gc}, given a desired (or at least reasonable) phase margin, φ_m. In this text, only the results needed to do the analysis of the system at hand will be given.

Consider a controlled linear system, where the plant model is given by the transfer function $G(s)$ and the controller by $C(s)$. The loop transfer function $L(s)$ is then given by $L(s) = G(s)C(s)$. The loop is closed by negative feedback, with the reference signal introduced as above. By examining the Bode plots for the open loop transfer function, $L(s)$, we can obtain information about the achieved performance for the closed loop system. We will use three well known relations to perform a simple analysis of the system, that will reveal fundamental limitations in achievable control performance.

- $|L(i\omega_{gc})| = 1$
- $\arg L(i\omega_{gc}) = -\pi + \varphi_m$.
- $\arg G(i\omega) = n\frac{\pi}{2}$
  where n is the slope of the function $\log|G(i\omega)|$. This approximate result is derived from Bodes relations, and is valid for minimum phase systems.

Now, we need the loop transfer function (in our case from $\dot{\varphi}_r$ to φ. We have

$$\begin{aligned} G(s) &= \begin{pmatrix} G_\theta \\ G_{\dot\theta} \\ G_{\dot\varphi} \end{pmatrix} = \begin{pmatrix} \dfrac{-71.23}{s^2 - 31.32} \\ \dfrac{-71.23s}{s^2 - 31.32} \\ \dfrac{191.2\ s^2 - 5947}{s(s - 31.32)} \end{pmatrix} \\ C(s) &= \bar{L} = \begin{pmatrix} l_1 & l_2 & l_3 \end{pmatrix} \end{aligned}$$

where the coefficients are taken from the system matrices in 8 This structure may be illustrated as in Figure 8, and the loop transfer function $L(s)$, from e to $\dot{\varphi}$ in the figure, may be derived;

$$L(s) = \frac{l_3 G_{\dot\varphi}}{1 + l_1 G_\theta + l_2 G_{\dot\theta}} = \frac{l_3(191.2\ s^2 - 5947)}{s(s^2 - 71.23 l_2\ s - 31.32 - 71.23 l_1)}. \qquad (10)$$

Notice that there is no pole-zero cancellation in the transfer function $G_{\dot\varphi}$, but the pole and the zero are very close. The characteristic polynomial contains a pure integrator, and l_1 and l_2 should be chosen to stabilize the states θ and $\dot{\theta}$.

Because of the stabilization, the unstable pole of the inverted pendulum appears as a zero in the transfer function from the reference to $\dot{\phi}$. This gives an upper limit to the achievable bandwidth of the closed loop system.

The method for determining performance constraints for non minimum phase systems presented in Åström (1999) suggests a factorization of the open loop transfer function into one minimum phase part and one non minimum phase part;

$$L(s) = L_{mp}(s)L_{nmp}(s).$$

The non minimum phase factor should have unit gain and negative phase. The condition for the phase margin then becomes

$$\begin{aligned} 0 &\geq -\arg L_{mp}(i\omega_{gc}) - \arg L_{nmp}(i\omega_{gc}) + \varphi_m - \pi \\ -\arg L_{nmp}(i\omega_{gc}) &\leq n\frac{\pi}{2} - \varphi_m + \pi \end{aligned}$$

where n is the slope of the gain curve at the cross over frequency. (n is assumed to be constant for feasible values of ω_{gc})

Now, in our case let us choose

$$L_{nmp}(s) = \frac{z-s}{z+s} = \frac{5.60-s}{5.60+s},$$

which gives

$$L_{mp}(s) = \frac{191.2l_3(s+5.60)^2}{s(s^2 - 71.23l_2s - 31.32 - 71.23l_1)}.$$

The phase of the transfer function $L_{nmp}(s)$ is

$$\arg L_{nmp}(i\omega) = -2\arctan\left(\frac{\omega}{z}\right).$$

Remains to determine the slope of the gain curve, n. As we can see, for low frequencies the transfer function $L_{mp}(s)$ is dominated by the integrator, for which the asymptote has the slope $n = -1$. However, the zeros at $z = -5.60$ implies a higher value of n. Let us assume that $n = -0.7$.

This gives us the following conditions for ω_{gc},

$$\begin{aligned} 2\arctan\left(\frac{\omega_{gc}}{z}\right) &\leq n\frac{\pi}{2} - \varphi_m + \pi \\ \frac{\omega_{gc}}{z} &\leq tan\left(n\frac{\pi}{4} - \frac{\varphi_m}{2} + \frac{\pi}{2}\right) \end{aligned}$$

If we require a phase margin of $\varphi_m = \frac{\pi}{3}$ we get the condition

$$\omega_{gc} \leq 0.54z = 3\ rad/s.$$

That is, we should not expect to obtain a closed loop system with higher bandwidth than 3 rad/s. Attempts to do this will inevitably decrease the phase margin. In the next section a Bode diagram for the transfer function system $L(s)$ can be seen. The controller has been obtained by LQ design, which guarantees a phase margin of $\frac{\pi}{3}$ when all states are available for feedback.

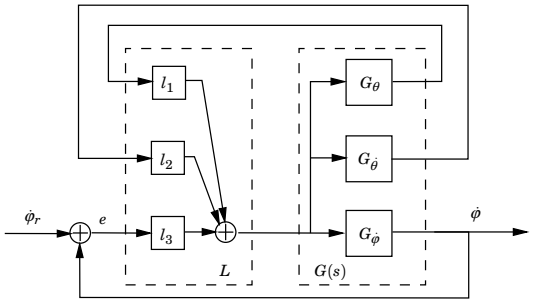

Figure 8 The state feedback controller.

4.4 A State Feedback Controller

To design the reduced order controller described above we have used LQ design, as in the stabilization case. In this design our objectives have changed, from just stabilize the pendulum, to controlling the velocity of the arm in addition to stabilization. That is, before we primarily penalized the θ and φ states, but now we are also interested in penalizing deviations in the controlled state $\dot\varphi$.

The design variables were selected as:

$$\begin{aligned} Q_{fb} &= \begin{pmatrix} 100 & 0 & 0 \\ 0 & 1 & 0 \\ 0 & 0 & 4 \end{pmatrix} \\ R_{fb} &= 80 \end{aligned}$$

yielding the state feedback vector

$$L = \begin{pmatrix} -7.6857 & -1.3676 & -0.2236 \end{pmatrix}$$

A Bode plot for the open loop system $L(s)$ may be seen in figure 9. As we can see, the phase margin is about $\frac{\pi}{3}$ radians, and the cross over frequency about 3 rad/s. These values are very much in line with the performance limitation results derived above.

A very critical feature of the linearized model is that it is highly dependent on the velocity $\dot\varphi_0$. This means that a controller calculated with the nominal model ($\dot\varphi_0 = 0$) is not likely to be successful in controlling the arm velocity for velocities different form zero. Our experiments confirm this reasoning; the control performance is poor if a constant feedback vector is used. Therefore we have made the design choice to schedule the control law with respect to $\dot\varphi$. Several feedback vectors were calculated, corresponding to arm velocities ranging from 0 to 20 radians per second (the design parameters Q and R were held constant). During the experiments the feedback vector was obtained at each sample through linear interpolation between the pre-calculated vectors. The interpolation is of course an approximation, but it proved to work well. The effect of the introduction of was dramatic, and the experiments would not have been nearly as well behaved without this feature.

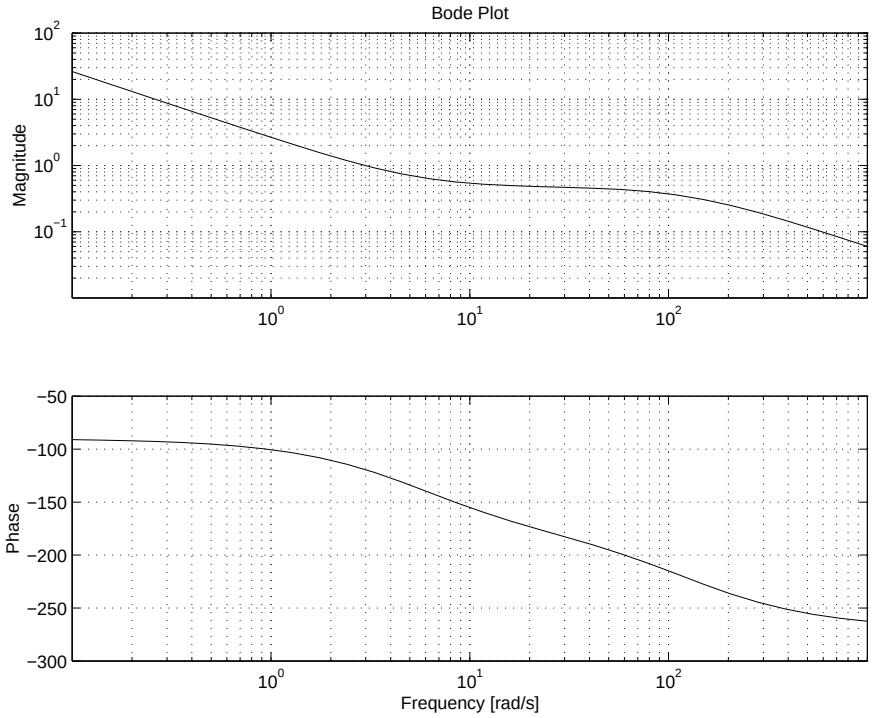

Figure 9 Bode diagram for the transfer function $L(s)$, see expression 10

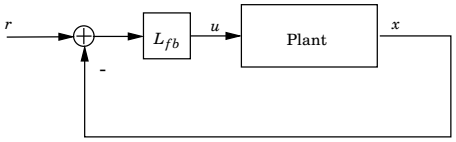

Figure 10 A feedback structure.

Gain scheduling does, however, come at a price; the controller is no longer linear. This complicates the analysis of the controlled system, by making it harder to apply linear theory.

4.5 Servo Mechanisms

As stated above, the problem we are considering is formulated as a reference following or servo problem. We would like the arm velocity of the pendulum to follow a specified trajectory. This problem may be solved in several ways, we will consider two common methods.

As a first attempt to solve the tracking problem, we will use a simple and straight forward technique where the the reference signal is introduced directly into the feedback loop, see figure 10. This yields the control law:

$$u = L_{fb}(r - x)$$

The main advantage of this method is its simplicity. It is easy to understand and implement, and is widely used. However, it has a few drawbacks. The most significant is that this strategy offers no possibility to separate the response to reference changes and disturbances. The result has to be

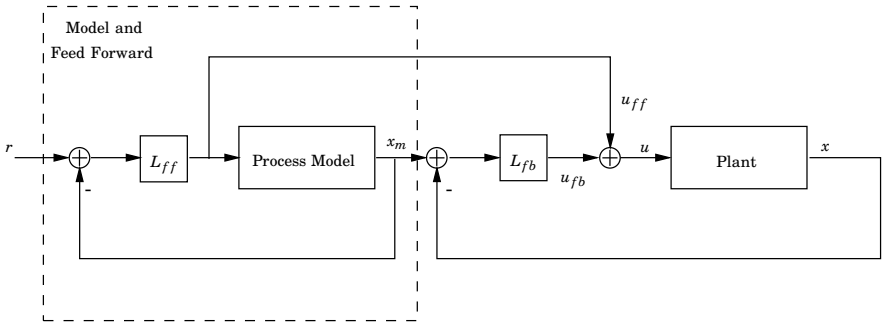

Figure 11 A feedforward structure.

a compromise. A better way of introducing reference signals is suggested in Åström and Wittenmark (1997). This structure is called a two degree of freedom controller, and may be seen in Figure 11. It consists of two controllers, one for feedback, and one for feedforward. The purpose of the feedback controller is to attenuate the effects of disturbances, model uncertainty, process variations etc. The robustness properties of the closed loop system is determined by the feedback design.

To solve the tracking problem, a feedforward controller is introduced. This controller has two missions; it should generate the feedforward control signal, and it should generate the expected state response for the given reference trajectory. The feed forward control signal drives the plant to the desired state, and would in fact be the only addition needed if the plant model and the plant itself were identical. Since this is never the case, the difference between the expected state response and the real state response is fed into the feedback controller. Differences between the model and the real plant is thereby taken care of by feedback, eliminating the need for a perfect plant model.

Such structure has the advantage of separating the regulating and tracking problems, enabling the designer to give different properties to the two different tasks. Feedforward is used to achieve performance and feedback to ensure robustness to process uncertainties and disturbances. It should be noted, however, that this controller structure does not necesarily imply better tracking performance, its strength is to separate control actions due to disturbances and reference changes respectively.

The feedback design is straight forward; a control law as the one in Section 4.2 could be used. The feedforward design leaves more freedom to the designer. We will use the strategy shown in Figure 11, where a plant model is controlled by state feed back. The resulting control signal and the state information from the controlled model is then used as described above. The remaining question is what model to use. A constant linear model will not be good enough, because of the fact that a linearized model is dependent on the arm velocity, $\dot{\varphi}_0$. One alternative would be to calculate several linear models and then interpolate during run time to obtain a valid model. It would also be possible use the nonlinear model directly (but then it would have to be discretized first).

To conclude, this approach to the tracking problem leaves us with the task

of designing two separated state feedback vectors, L_{fb} and L_{ff}. In the experiments, the same L_{fb} as before was used and L_{ff} was calculated using LQ design with weighting matrices:

$$\begin{aligned} Q_{ff} &= \begin{pmatrix} 100 & 0 & 0 \\ 0 & 1 & 0 \\ 0 & 0 & 4 \end{pmatrix} \\ R_{ff} &= 30 \end{aligned}$$

yielding the state feedback vector

$$L = \begin{pmatrix} -8.2802 & -1.4732 & -0.2438 \end{pmatrix}$$

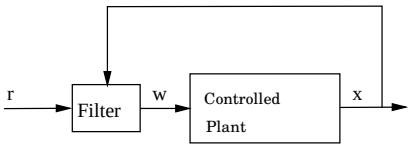

Figure 12 A nonlinear controller structure

5. Safe Manual Control

Now that we have established the necessary framework needed to perform manual control, we shall focus on the critical problem addressed in Section 2, namely reference following in the presence of saturating actuators.

The control mission was defined as controlling the the arm velocity, $\dot{\varphi}$, while keeping the pendulum in upright position. Under these circumstances, there are two conflicting objectives, namely, accurate tracking and preserved stability of the pendulum. These contradictory tasks, in combination with limited control authority captures the core of the problem that will be discussed in the following.

Stability is a property of a solution of a differential equation, or a set of differential equations. This fact has two important consequences. First, a system can in general not be classified as stable or unstable. Second, the system equations has to be considered in combination with the initial conditions. Linear systems however, is an exception. For those, stability is a property of the system as well as its solutions. When we introduce a control signal saturation, the system is no longer linear, and we have to consider the initial conditions as well as the system equations. This distinction is crucial. In our application, it means that there exists reference trajectories which destabilize the system, if no protection mechanism is used. The control design mission may, with this insight, be stated as designing a controller that stabilizes the system independently of the reference signal. See also the example in Section 2).

We will start by designing a nonlinear controller justified by intuitive reasoning. As a more formal attempt to gain insight into the problem, we will discuss a design method based on admissible set theory and saturation avoidance. This strategy focuses on saturation avoidance, and might be unnecessarily conservative. With this motivation we will engage a phase plane analysis of the inverted pendulum system, where the consequences of the saturating input is considered. This analysis will result in an alternative controller structure.

This section deals with the linearized pendulum model. The (possibly questionable) assumption is that the controllers developed here will, with some modifications, be efficient also when applied on the real pendulum.

5.1 A Heuristic Approach

The feedback and the feedforward controllers described in section 4.5 do not address the problem of saturating control signal input. A sufficiently large step in the reference signal will drive the system unstable (See figure 13). As an attempt to cure this problem, we introduce heuristically a

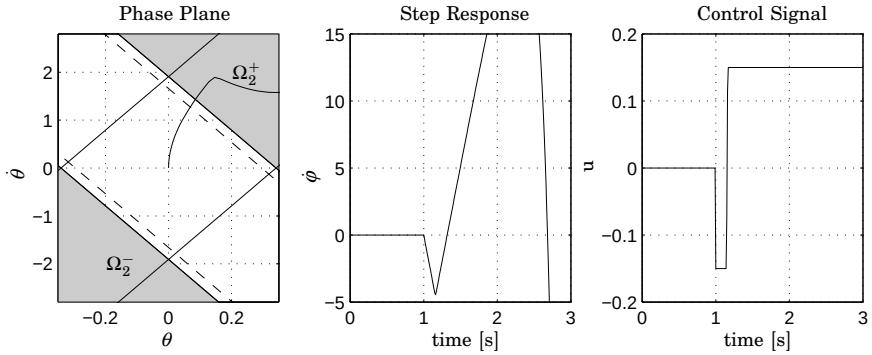

Figure 13 Simulated response to step reference change in $\dot{\varphi}$. No protection mechanisms is used, and stability is lost. The regions Ω_2^+ and Ω_2^- represents unstable regions for the system and will be derived and discussed in the following.

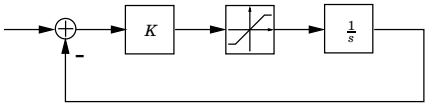

Figure 14 A rate limiter structure.

filter applied to the reference signal $\dot{\varphi}_r$ before it is fed into the system, see figure 12. Since the dimension of the reference signal is velocity but the control signal represents an acceleration (the derivative of the velocity), it is reasonable to focus on changes in the reference. If friction is neglected, the control signal is zero when the system is in steady state, for example when the pendulum is upright and the arm is rotating with constant velocity. Abrupt changes in the velocity reference may however, lead to large control signals, possibly saturating. In this situation the control loop is in effect broken, and stability might be lost. This leads us to the idea of using a rate limiter applied on the reference signal to restrict the rate of change in the reference. The rate limiter used here is presented in Rundqwist *et al.* (1997), see fig 14, which provides not only rate limiting, but also a filtering of the reference signal. The parameter K may be used to tune the filtering effect. This strategy may be implemented so that stability is preserved by setting the maximum rate (adjusting the saturation levels in figure 14) sufficiently low. This is, however, quite conservative. A better approach would be to let the limits of the rate limiter be adaptive, changing with the states of the pendulum. It is reasonable that the maximum rate of change in the reference, that does not drive the pendulum out of stability, depends on the states of the pendulum, primarily the pendulum angle and the angular velocity. Introduce

$$\beta = \theta + k\dot{\theta}$$

where k is chosen so that the weighting between the states is fair. Further, β is used to determine how fast the reference signal is allowed to change. That is, β represents the maximal rate of the rate limiter. A large value of $|\beta|$ indicates need of stabilization, the limit should therefore be set tight in this case. Small β indicates that the pendulum is far from instability, and faster changes in the reference signal can be allowed.

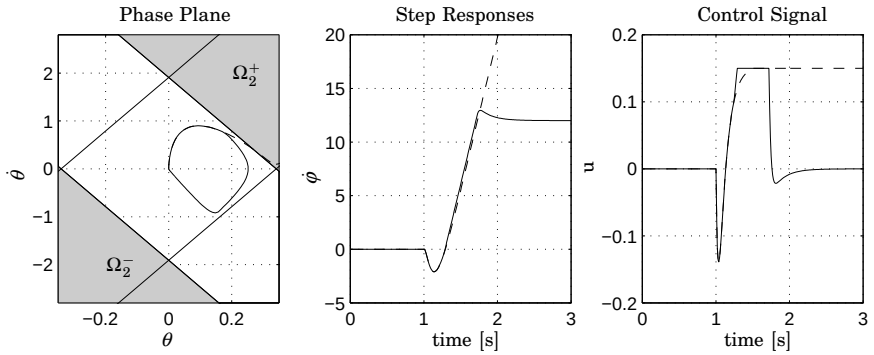

Figure 15 Simulated responses to step reference change in $\dot{\varphi}$. The rate limiter is tuned to achieve a good response to a 12 rad/s, but fails to produce a stable response to a 18 rad/s step.

The mapping from β to the rate limiter can be done in many ways. The function used in the experiments was

$$\gamma = k(1 - |\beta|)$$

where γ is the rate limiter limits and k the maximum rate of change. It is here assumed that β is scaled and so that $|\beta| < 1$.

Using this approach and tuning the parameters of the reference signal filter, it was possible to use the control feedback vector derived in Section 4.2. In Figure 15 Simulations of system response to step changes in the reference can be seen. As we can see, it is possible to tune the rate limiter so that a well behaved response is achieved for a particular step size. This rate limiter might however fail to ensure a stable response to other, bigger steps. Numerical values used in the simulations were $\beta = 1$ and $k = 45$.

5.2 Admissible Sets and the Reference Governor

The rate limiter strategy discussed in the section above has good intuitive interpretations. However, no stability results were presented. On the contrary, it was shown that the filter could be tuned to give well behaved responses for some reference trajectories, but fail for others. This is of course highly undesirable.

In this section we will use the same controller structure as in figure 12, but the filter unit (the mapping from r to w) will be based on a strong theoretical foundation. The strategy is based on the theory of maximal output admissible sets and the reference governor, presented in Gilbert and Tan (1991) and Gilbert *et al.* (1994). The theory of admissible sets and its most important results are summarized in Appendix B. This section differs from the rest of the text in the sense that a discrete time formulation will be used instead of continuous time.

Consider the discrete time version of the system 8 discretized with sampling interval $h = 10\ ms$

$$\begin{aligned} x_{k+1} &= A_d x_k + B_d u_k \\ u_k &= -L_d(x_k - w_k^c). \end{aligned}$$

yielding the closed loop system

$$x_{k+1} = (A_d - B_d L_d)x_k + B_d L_d w_k^c = Ax_k + B^c x_k.$$

It is here assumed that the reference signal, w_k, is introduced directly into the feedback loop. Since $w_k^c = (0\ 0\ w_k)^T$ in this particular case, the system may be simplified to

$$x_{k+1} = Ax_k + Bw_k \tag{11}$$

where

$$B^f = (B_1\ B_2\ B)$$

We shall now apply the design method from Appendix B. First, we need to define the control signal saturation. Let

$$y_t = u_t = -Lx_k + l_3 w_k = Cx_k + Dw_k \in Y = [-u_{sat}, u_{sat}]$$

where

$$L = (l_1\ l_2\ l_3)$$

This gives us the extended system with the reference governor included,

$$\begin{aligned} x_{k+1}^G &= A_G x_k^G + B_G K(r_k, x_k^G)(r_k - (I\ 0)x_k^G) \\ y_k &= C_G x_k^G \ \in Y \\ x_k^G = \begin{pmatrix} w_k \\ x_k \end{pmatrix},\ A_G &= \begin{pmatrix} 1 & 0 \\ B & A \end{pmatrix},\ B_G = \begin{pmatrix} 1 \\ 0 \end{pmatrix},\ C_G = (l_3\ -L), \end{aligned} \tag{12}$$

which is equivalent to system 20. The admissible set for y_k is then given by

$$\begin{aligned} Y &= \{y : f_i(y) \leq 0,\ i = 1, 2\} \\ f_1(y) &= y - u_{sat} \\ f_2(y) &= -y - u_{sat}. \end{aligned}$$

The first task is to calculate the maximal admissible set, $O_\infty(A_G, C_G, Y)$. In doing this, we use the algorithm given in Appendix B. Since the constraints are linear, the calculations are quite simple and easily carried out in Matlab. The result of the calculations are shown in figure 16. The admissible set is a subset of $\Re^4$, but since $y_k = u_k = l_1\theta + l_2\dot{\theta} + l_3(w - \dot{\varphi})$ it is reasonable to consider $w - \dot{\varphi}$ instead of w and $\dot{\varphi}$ separately. After this transformation the dimension of the set is reduced to $\Re^3$, which makes it easier to visualize. In the figure, three level curves of the system can be seen, for $\dot{\varphi} = 0$, $\theta = 0$ and $\dot{\theta} = 0$ respectively. An important observation is, although it cannot be seen in the figure, that the set is closed. This is critical, since we otherwise would risk loosing stability even if the state of the system was contained in the admissible set. The origin is also contained in the the admissible set, which is of course essential.

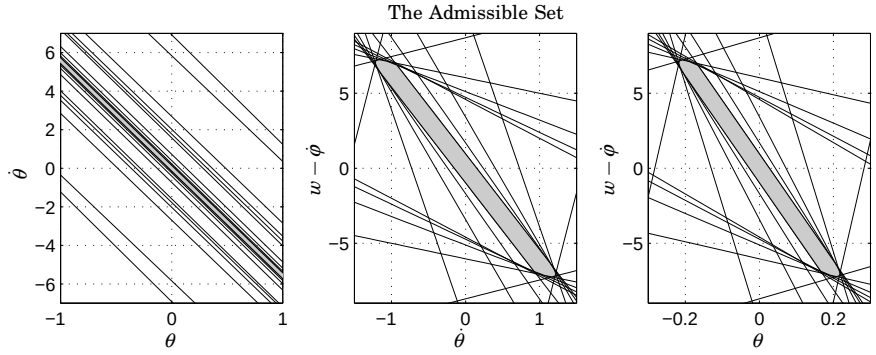

Figure 16 The admissible set resulting from the algorithm given in Appendix B. The gray areas represents the admissible set. In the first plot, $\dot{\varphi}$ is assumed to be zero, in the second, $\theta = 0$ and in the third $\dot{\theta} = 0$.

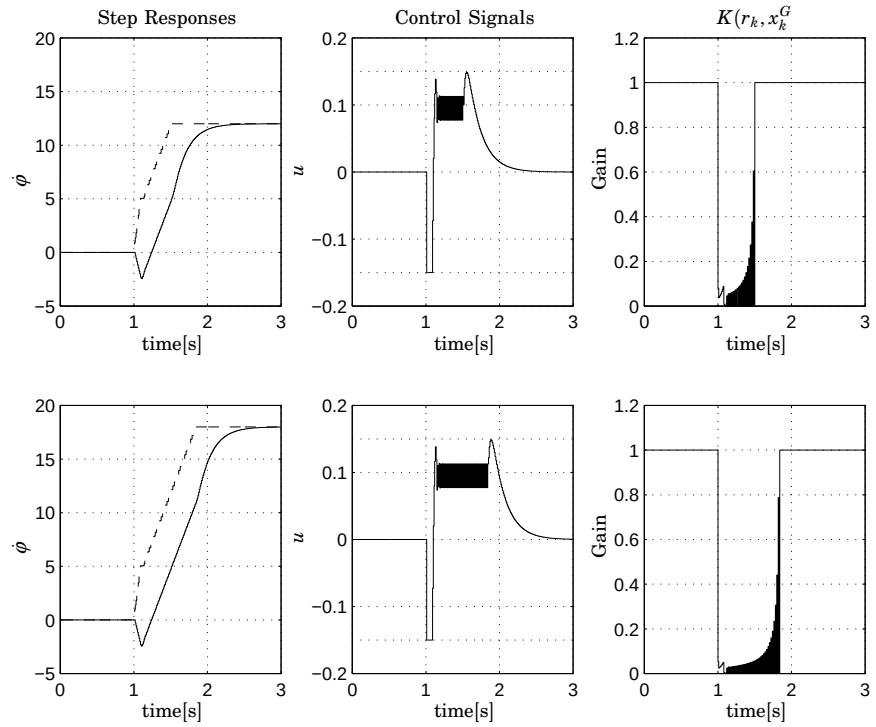

Figure 17 Simulations of the linearized pendulum system when controlled by the reference governor. Above, a step from 0 to 12 rad/s is applied, below, a step from 0 to 18 rad/s. The dashed line is the filtered reference signal w. Notice the chattering effect in the control signal. Saturation limits are dotted in the control signal plot.

We are now ready to put it all together and simulate the reference governor based controller. In doing this we skip one design step that might be of importance if the controller was to be implemented on a real system. That is, finding a simple (approximate) representation of the admissible set $O_\infty(A_G, C_G, Y)$. For simulations however, the controller strategy described in Appendix B is sufficient.

Figure 17 shows simulations of the reference governor. Two steps in r_k

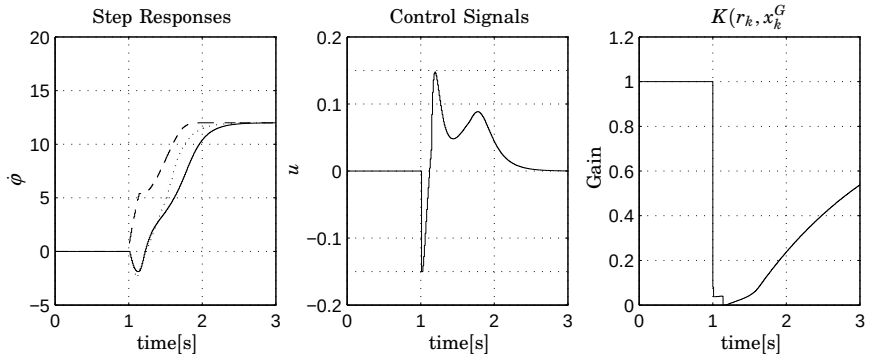

Figure 18 The effect of filtering the reference governor gain. The step response (solid) is somewhat slower that without gain filtering (dotted). The signal w_k (dashed) is also shown. Notice that the chattering is entirely eliminated.

are shown. The output of the reference governor, w_k, is plotted (dashed) together with the responses (solid). The filter gain, $K(r_k, x_k^G)$, is unitary most of the time, but becomes significantly smaller when there is a risk of violating the control signal constraint. The responses are well behaved, and the reference governor is successful in preserving the stability of the system.

Even if this controller successfully solves the problem of stabilization, there is chattering in the control signal. This is not much of a problem in the simulations, but is highly undesirable in a real system. To solve this problem, we suggest that the gain $K(r_k, x_k^G)$ is filtered before it is used by the reference governor. This filtering has to be done with caution. When modifying K, there is an obvious risk that we do it in a way that leads to violation of the constraints. With this in mind, we suggest the following filter for $K(r_k, x_k^G)$

$$K_k^f = \begin{cases} K_{k-1}^f + \beta(K_k - K_{k-1}^f), & K_f - K_{k-1}^f \geq 0 \\ K_k, & K_f - K_{k-1}^f < 0 \end{cases}$$

where $K(r_k, x_k^G) = K_k$. The resulting signal, $K^f(r_k, x_k^G) = K_k^f$ is then used by the reference governor. The filter is devised so that negative gain changes are directly propagated to the reference governor. Such changes are critical, since they imply that restrictions has to be made in order to avoid violating the constraints. If the gain is increasing, however, low pass filtering is performed. This is also in line with the observations in figure 17. The chattering is present when the reference governor gain is increasing.

In Figure 18 the effect of the gain filtering is shown. The response is somewhat slower that before, but the control signal is now well behaved.

The design method in this section is supported by strong theoretical results. Also, it has proven itself successful in simulations, as shown above. However, the method relies very much on the ability to predict the behavior of the system, also for long time horizons. This implies that the method might be sensitive to modeling errors. It is thus fair to suspect that the application of the reference governor to a real plant might be troublesome,

especially if the plant model is not very good. Prediction of friction behavior is particularly troublesome in our case.

5.3 A Phase Plane Analysis of the Pendulum Behavior

So far we have looked at strategies that strive to avoid saturation, an interesting question is to investigate what happens if we allow saturation. Phase plane analysis will be used to find the answer. We will study the linearized system (8) in detail, and also discuss the validity of the obtained results for the nonlinear plant.

Stability is essentially determined by only two states; $x_1 = \theta$ and $x_2 = \dot{\theta}$. The dynamics for these states are described by (using the linearized model),

$$\begin{aligned} \dot{x}_1 &= x_2 \\ \dot{x}_2 &= \alpha x_1 + \beta u \end{aligned} \tag{13}$$

Now, assume a control law on the form

$$u = \text{sat}_{u_{sat}}(-l_1 x_1 - l_2 x_2).$$

where $\text{sat}_{u_{sat}}$ denotes a function that saturates at $\pm u_{sat}$. The controller gains l_1 and l_2 are chosen to stabilize the system. When $|u| \leq u_{sat}$ the system operates linearly, and is then stable. The interesting question is how the system behaves when the control saturates, i.e. $|u| > u_{sat}$. To answer this question, let us examine the phase plane of the system.

When the control signal saturates, the system is described by

$$\begin{aligned} \dot{x}_1 &= x_2 \\ \dot{x}_2 &= \alpha x_1 \pm \beta u_{sat} \end{aligned}$$

with two equilibria at

$$\begin{aligned} (x_1^{eq}, x_2^{eq}) &= (p, 0) = \left(-\frac{\beta u_{sat}}{\alpha}, 0 \right). \\ (x_1^{eq}, x_2^{eq}) &= (-p, 0) = \left(\frac{\beta u_{sat}}{\alpha}, 0 \right). \end{aligned}$$

Further we can conclude that the equilibrium points are unstable, since the system matrix has the eigenvalues $\lambda_1 = \sqrt{\alpha}$ and $\lambda_2 = -\sqrt{\alpha}$. To reveal the qualitative behavior of the system, consider the following expressions;

$$\begin{aligned} \ddot{\theta} &= \alpha\theta \pm \beta u_{sat} \\ \dot{\theta}\ddot{\theta} &= \alpha\dot{\theta}\theta \pm \beta u_{sat}\dot{\theta} \\ \frac{1}{2}\frac{d}{d\theta}\dot{\theta}^2 &= \frac{1}{2}\alpha\frac{d}{d\theta}\theta^2 \pm \beta u_{sat}\frac{d}{d\theta}\theta \\ \frac{1}{2}\dot{\theta}^2 &= \frac{1}{2}\alpha\theta^2 \pm \beta u_{sat}\theta + C \\ 0 &= \alpha\left(\theta \pm \frac{\beta u_{sat}}{\alpha}\right)^2 - \dot{\theta}^2 - \frac{\beta^2 u_{sat}^2}{\alpha} + C \end{aligned}$$

where the last expression describes a hyperbolic function.

Figure 19 shows the behavior of the system (13). In the figure, the axes for the hyperbolic trajectories can be seen, as well as the lines $u = 0$ (solid, goes through origo), $u = u_{sat}$ (dashed) and $u = -u_{sat}$ (dashed). We can also see that the state trajectories are stable for some initial conditions, but diverges for others. That is, the phase plane is divided into stable, and unstable regions.

In the plot, five different regions are marked, corresponding to different modes of operation.

- Ω_0
  In this region the system operates linearly, i.e. the control law is
  $$u = -l_1 x_1 - l_2 x_2.$$
  The region is determined by the lines $u = u_{sat}$ and $u = -u_{sat}$.
- Ω_1^+
  The control signal saturates, $u = u_{sat}$. The region is bounded from below by the line $u = u_{sat}$ and from above by one of the hyperbolic axes corresponding to the right equilibrium. Notice that these lines doesn't have to be parallel. However, the LQ controller designed used to obtain L appeared to yield lines very close to parallel. The most significant characterization of this region is that the solutions are stable; trajectories starting in Ω_1^+, converges to origo.
- Ω_1^-
  Equivalent to Ω_1^+, but bounded by the lines $u = -u_{sat}$ and a hyperbolic axes corresponding to the left equilibrium.
- Ω_2^+
  Also in this region the control signal saturates. The difference from Ω_1^+ and Ω_1^- is that trajectories in this region are unstable.
- Ω_2^-
  Equivalent to Ω_2^+; unstable.

To conclude, we have shown that the phase plane may be divided into one stable region and two unstable. An important observation is that saturating control inputs does not necessarily cause instability, and that the stable region is significantly larger that the one implied by the saturation limits.

Let us now discuss the consequences of introducing also the state $x_3 = \dot{\varphi}$ in the model,

$$\begin{aligned} \dot{x}_1 &= x_2 \\ \dot{x}_2 &= \alpha x_1 + \beta u \\ \dot{x}_3 &= \gamma x_1 + \varepsilon u \end{aligned} \tag{14}$$

The control law is now assumed to be

$$u = \mathrm{sat}_{u_{sat}}(-l_1 x_1 - l_2 x_2 - l_3 (x_3 - r)).$$

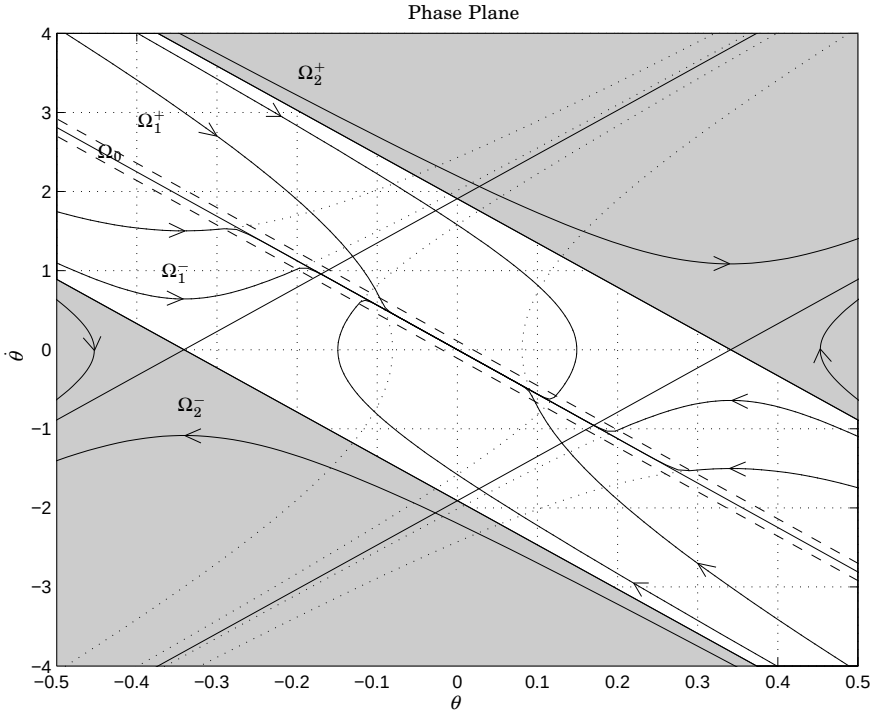

Figure 19 Phase plane for the constrained system (13). The solid curves are actual state trajectories. The dotted curves represent the hyperbolic extensions of the state trajectories. The dashed lines marks the saturation limits. The important conclusion to be drawn from this phase plot, is that the state space is divided into a stable region (unshaded) and two unstable regions (shaded).

Since we as far as stability is concerned still only consider the states x_1 and x_2, we continue to analyze the phase plane for these variables. However, we shall now examine the resulting system behavior when x_3 is introduced in the control law.

First we notice that the two hyperbolic trajectory sets analyzed above are not altered. The saturation lines however, will be dependent on the value of the state x_3. The expression for the saturation lines are

$$x_2 = \frac{1}{l_2}(\pm u_{sat} + l_1 x_1 - l_3(x_3 - r)).$$

This corresponds to a planes in (x_1, x_2, x_3) space, and if a constant $x_3 - r$ is assumed, lines in (x_1, x_2) space. Different values of $x_3 - r$ forces the region Ω_0 to move vertically. By studying Figure 19 we see that this is critical. The location of region Ω_0 governs which trajectory set is active. If, for example the upper limit of Ω_0 is located in Ω_2^+ (i.e. Ω_1^+ is eliminated) the system will inevitably be put in a state which is not recoverable, and stability is lost. Now, this means that enforcing stability is the same as always enforce existence of the regions Ω_1^+ and Ω_1^-.

With this insight, we are ready to suggest a controller for the system 14 that stabilizes the system for all possible changes in the reference value r. The troublesome term in the control law, and also the one that has to be

restricted, is $-l_3 x_3$. Introduce

$$u^c = -l_3(x_3 - r)$$

and the revised control law

$$u = \text{sat}_{u_{sat}}(-l_1 x_1 - l_2 x_2 + \text{sat}_{u^c_{sat}}(u^c)).$$

This control law offers the possibility to restrict u^c, in such way that the regions Ω_1^+ and Ω_1^- always exist in the phase plane. This yields a stable closed loop system from r to x.

This control strategy using cascaded saturations is well known and documented in the literature. An example of its applications is given in Burg *et al.* (1996).

It now remains to calculate admissible values for u^c_{sat}. The condition for guaranteed stability is, as stated above, equivalent to the existence of the regions Ω_1^+ and Ω_1^-. The situation may be illustrated as in Figure 20. For simplicity we assume that the border line between Ω_1^+ and Ω_2^+ and the $u = u_{sat}$ are parallel. Also assume that we desire a safety margin for stability, and call it Δ. Introducing

$$q = \frac{\beta u_{sat}}{\sqrt{\alpha}}$$

gives us an upper bound for u^c_{sat}:

$$u^c_{sat} < -l_2(q - \Delta) - u_{sat}$$

In Figure 21 the effect of the proposed control strategy may be studied. In the simulations, a linear model was used. The state feedback vector L, was the one derived in section 4.2. The design parameter Δ, was set to 0.25. In the upper plots in the figure, responses to reference steps in $\dot{\varphi}$, when u^c is constrained, are shown. As we can see, the responses are well behaved for different step sizes, and that the critical states θ and $\dot{\theta}$ never leaves the specified region. The lower plots shows the system response when u^c is not restricted. As we can see, the control signal saturates and drives the system outside the stability region.

The controller structure presented here, is similar to one suggested in Brufani (1997). The controller developed there, distinguish between stabilizing control (for x_1 and x_2) and reference following control (for x_3). In order to preserve stability, the control law responsible for reference following is restricted in the same manner as in the control law discussed above. In Brufani (1997), a more restrictive approach to saturating control signals is taken than in our analysis, which might lead to somewhat conservative controllers. It should be said however, that Brufani (1997) discusses control of nonlinear systems as well as linear, whereas we have limited our analysis to the linearized case.

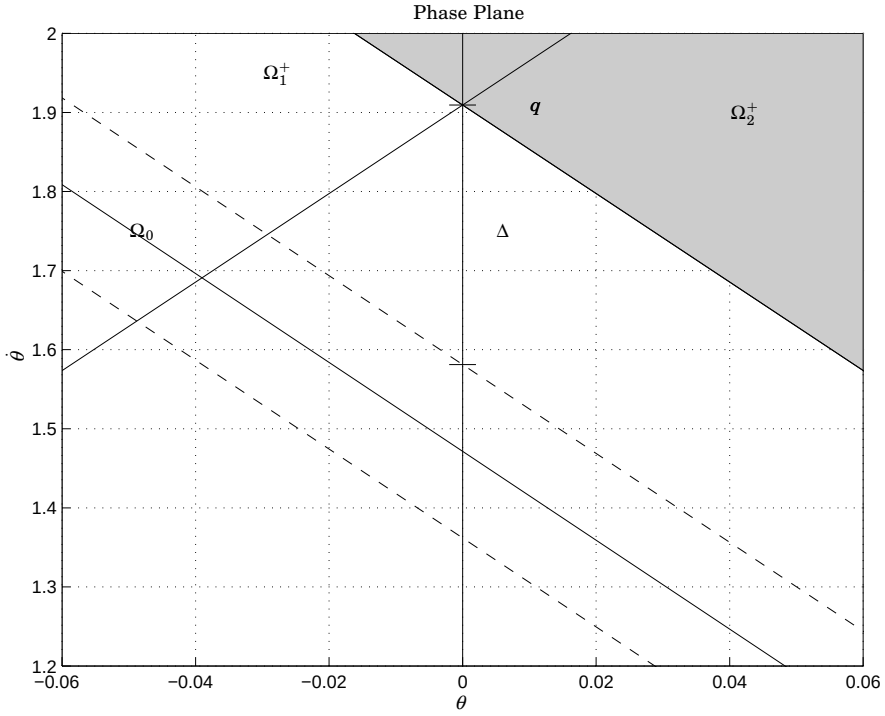

Figure 20 Calculation of admissible u^c_{sat}. Δ may be used to obtain desired width of the region Ω_1^+.

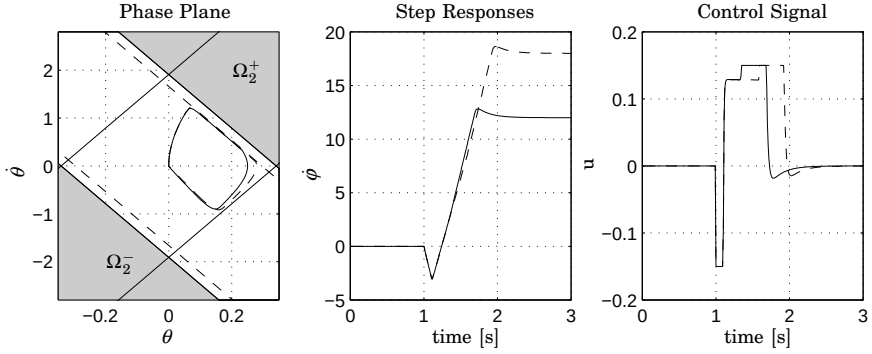

Figure 21 Simulated responses to step reference change in $\dot{\phi}$. Above, constrained ($|u^c| < u^c_{sat}$) responses for steps from 0 to 12 rad/s and 18 rad/s respectively. Both responses are well behaved.

5.4 Summary

Three different controllers, and two versions of one of them, have been derived and simulated in this section. A linearized pendulum model has been used in the design procedures. This approximation, and its implications, will be discussed further in Section 6. The design objective has been to construct safe, (i.e. yielding a stable closed loop system) but high performing controllers (as discussed in section 4.1). The three controllers all have different motivations; the rate limiter controller is based on heuristic reasoning, the reference governor strives to avoid saturation, whereas the cascaded saturations controller explores the behavior of the system oper-

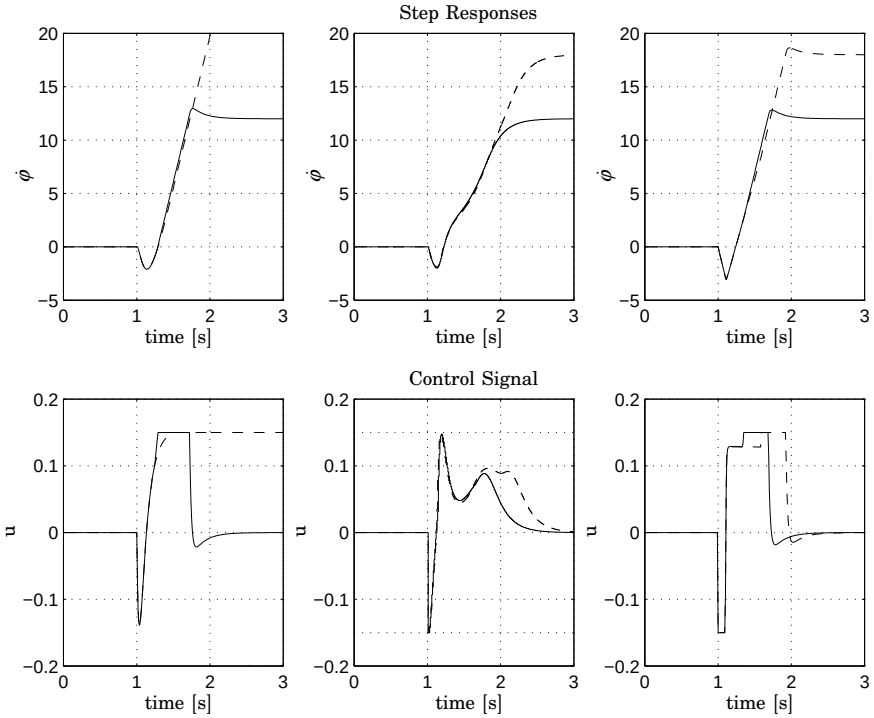

Figure 22 Simulated responses and control signals for the rate limiter controller (left), the reference governor (middle) and the cascaded saturations controller (right). The solid and dashed curves represents responses to 12 rad/s and 18 rad/s input steps respectively. The filtered gain version of the reference governor was used for the simulations in this figure.

ating in saturation. As we have seen, all controller structures can be used to solve the problem. However, they have their own individual strengths and weaknesses, which we shall now discuss.

The rate limiter based controller has a simple structure, and good intuitive interpretations. It also assumes little knowledge about the system, which might be an advantage. A serious disadvantage is, however, that it does not necesarily yield global stability. The rate limiter controller may be tuned to give good performance for a certain step size, but then fail to stabilize the system for larger steps. (See Figure 22.)

The reference governor relies on a solid theoretical foudation. Global stability results are available, which makes the approach particularly interesting. The theory of admissible sets is also attractive because of its generality; it is applicable to a large class of constrained linear systems. Simulations of the reference governor (see Figure 22) shows well behaved responses, for various stepsizes. The control signal chattering apparent in simulations of the original formulation of the reference governor, may, as we have shown, be suppressed at the cost of slightly degraded performance. However, in spite of the promising theoretical results, the reference governor has one potentially severe drawback. It relies on the ability to predict the system behavior for long time horizons. This might be a serious problem if the system model poorly resembles the real plant. This issue will be discussed further in the next section.

Finally, there is the cascaded saturations controller. Also this controller yields a globally stable closed loop system. The means for achieving this is however fundamentally different from the approach taken by the reference governor. Instead of striving to avoid saturation, this controller explores and uses the saturated behavior of the system. Simulations of the controller (see figure 22) shows fast and well behaved responses. However, this controller structure has at least two drawbacks. Firstly, it presumes thorough knowledge about the system. This might lead to problems if the plant model is uncertain. Secondly, it lacks generality. An essential part of the design is a phase plane analysis of the constrained system. This analysis has to be done individually for each system to be controlled, and it also scales badly to systems of higher order.

6. Experiments

One of the objectives in this work was to implement a well working control strategy for a real Furuta pendulum. This task proved to be very challenging, and much time has been spent on designing an efficient control system for the real Furuta pendulum. Various problems, for example friction (as discussed in Section 3.4), noise and nonlinearities made the implementation far from straight forward. (A description of implementational details is given in Section 8).

When applying a control strategy designed for a linear model to a real plant as in our case, the potential difference between the model and the plant may be a source of problems. This application is no exception. The nonlinear model captures the basic pendulum dynamics, but higher order dynamics (for example an oscillatory mode appearing in the somewhat flexible pendulum) is neglected. Further, even more dynamic behavior is lost in the linearization. The gain scheduling with respect to arm velocity helped, but not fully. We have also experienced difficulties when attempting to use observers for estimation of the velocity states $\dot{\theta}$ and $\dot{\varphi}$ from measurements of θ and φ. This result (discouraging enough not to be presented) was primarily due to noise and friction. The problem was solved using analog filters to obtain the derivatives.

A characteristic feature of all experiments presented in this section was that many of the parameters involved in the controllers had to be tuned iterativley, in order to get good results. Some of the parameters also had to be readjusted between the experiments, or even during experiments, due to small changes in the process. (Friction changed with the temperature and the wear of the slip rings.)

The compromise between stabilization and manual control is easier to resolve when the system has high control authority. Our experimental equipment allows an acceleration of the pivot point of about $\pm 2\ g$. In our experiments the acceleration was restricted to $\pm 0.5\ g$, to make the problem more difficult. With this saturation limit, a controller without protection mechanisms failed to stabilize the system when a $12\ rad/s$ step in $\dot{\varphi}_r$ was applied. To enforce a safe control strategy, the methods presented in section 5.1 and Section 5.3 were implemented and tested on the real pendulum.

A mentioned above, quite a few controller parameters had to be adjusted in order for the strategies to work. Results valid for the linearized system worked poorly on the real pendulum without some modifications. The changes however, did not alter the principal controller structures, but rather forced the controllers to be a bit less aggressive.

The implementation of the rate limiter was straight forward. There are two parameters to tune for best performance, β and k. When the saturation limits has been set, only a few iterations were required to determine values of β and k that yields a system with good behavior. The results may be seen in Figure 23 and 24. A we can see, the step responses are well damped, with settling times of about $2.5\ s$ for steps from $12\ rad/s$ to $-12\ rad/s$. If we look at the control signal (Figure 24) we can see that the control signal saturates at certain points.

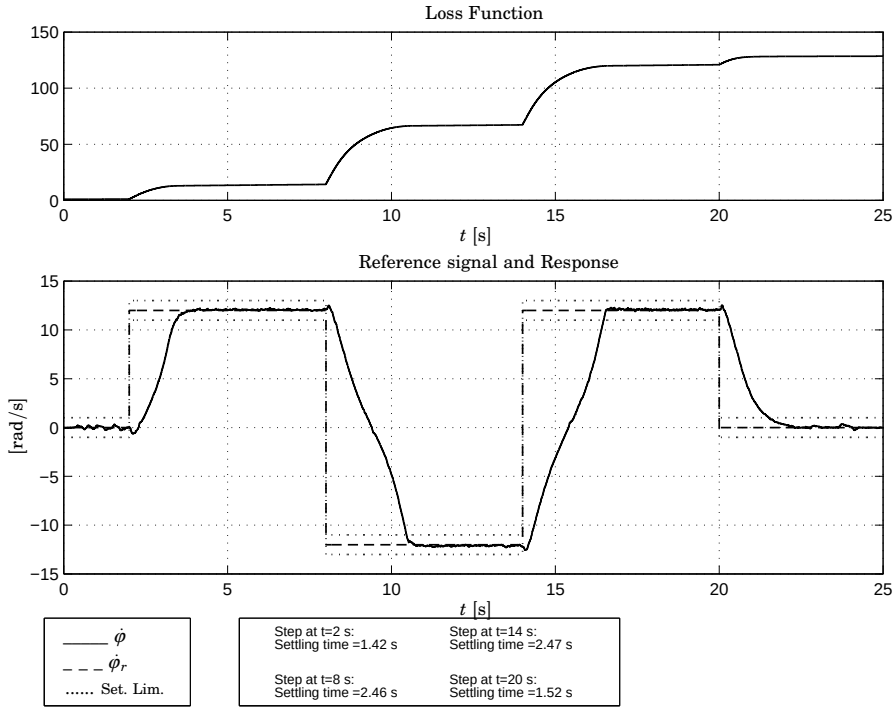

Figure 23 Step responses when the rate limiter controller was used.

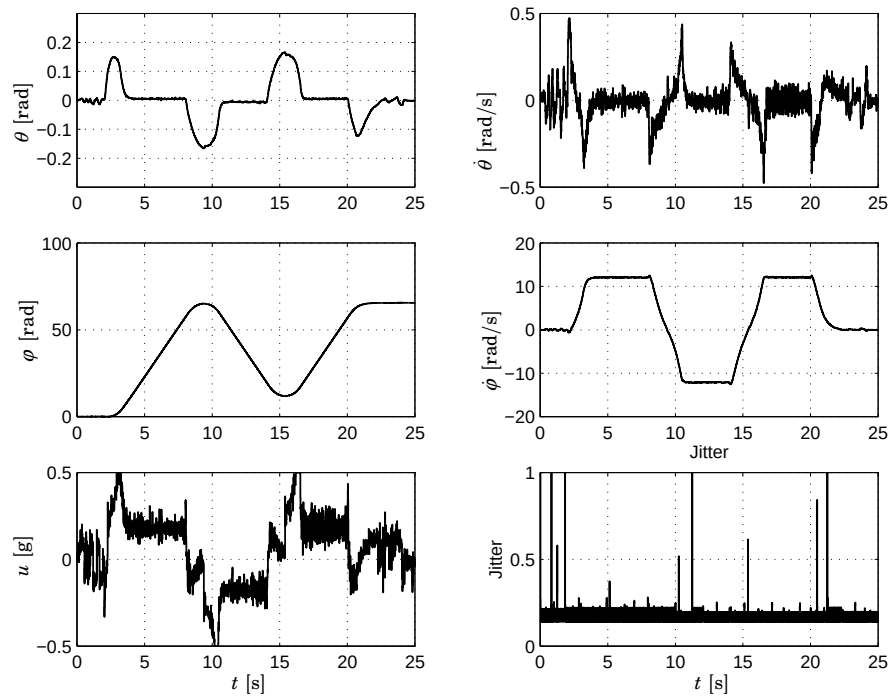

Figure 24 State measurements, control signal and jitter curve for the rate limiter experiment. The jitter shows what fraction of the sampling interval the computer uses for calculations.

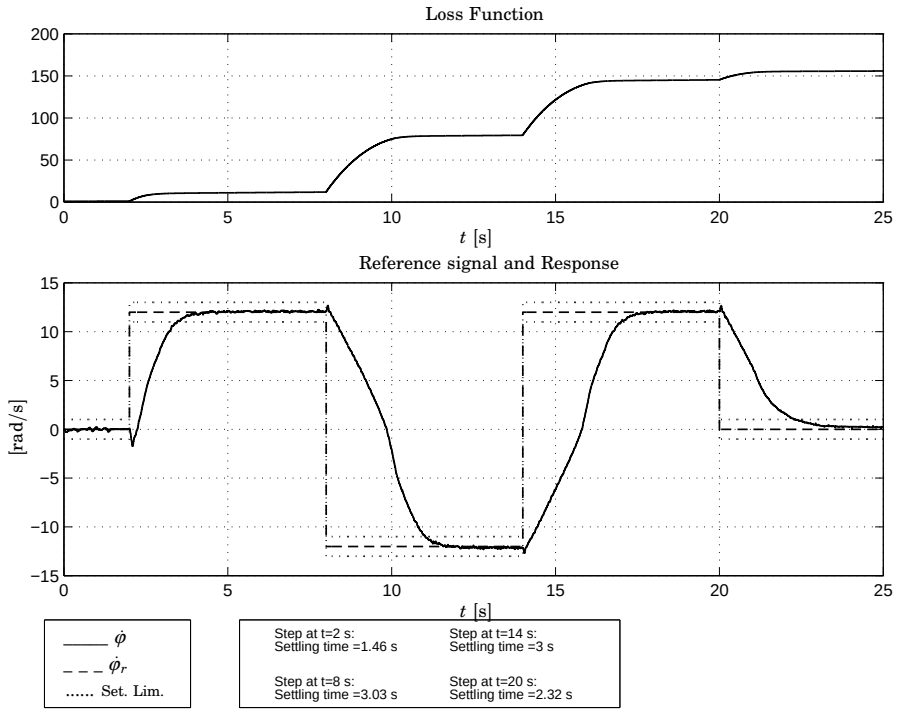

Figure 25 Step responses when the cascaded saturations controller was used.

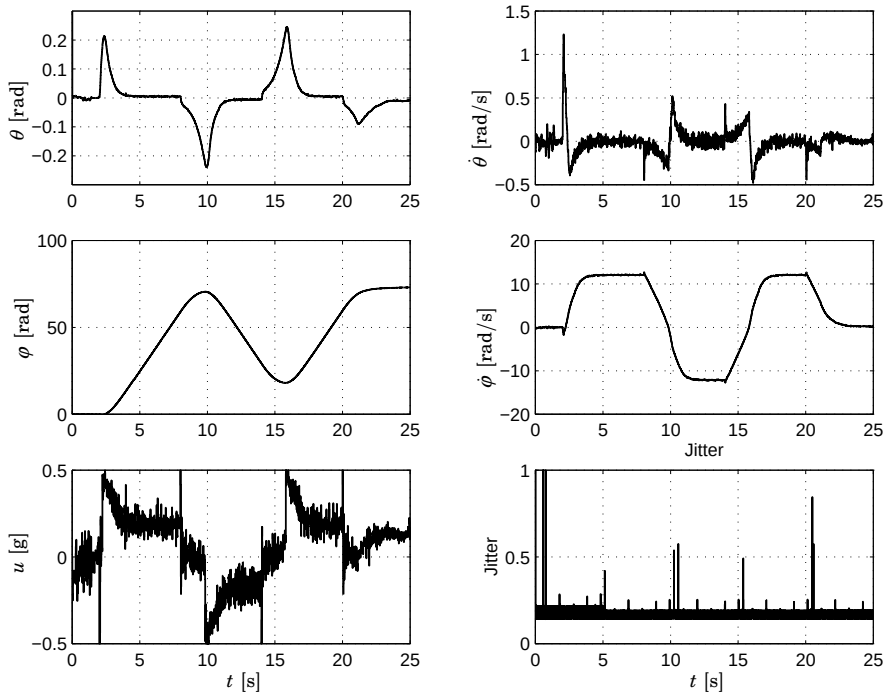

Figure 26 State measurements, control signal and jitter curve for the phase plane controller experiment.

The situation was a little more complicated for the phase plane controller. First, the saturation limit u_{sat}^c depends on the linearized model and should thus be gainscheduled in the same manner as the state feedback vector. However, this modification was not sufficient. The value u_{sat}^c also depends on the actuator saturation limit u_{sat}, which is different from the effective saturation in the presence of friction and friction compensation. The value of u_{sat}^c had to be scaled down in the design. A third modification that was made in the design was to add a constant term to the signal that was used for gain scheduling the state feedback vector. That is, a higher arm velocity was assumed for gain scheduling. With these modifications, the controller achieved the result in Figure 25. The settling times are slightly higher than for the rate limiter controller. The reasons for this is not entirely clear to us, but some suggestions are given in the following section.

To summarize the experiments, both the rate limiter controller and the controller based on the phase plane analysis worked on the real pendulum. However, the controller parameters had to be tuned to some extent.

7. Results and Conclusions

In this thesis, we have investigated the behavior of an unstable system subject to manual control, in the presence of control signal saturation theoretically and practically. The inverted pendulum has served as an illustrative example for the analysis and design as well as the the experimental part of this work. In this section the major results are summarized, and some possible extensions suggested.

7.1 Theoretical Results

Three different protection mechanisms were discussed in Section 5; a heuristic approach, a reference governor and a controller based on cascaded saturations. The three controllers all have different motivations, and focuses on different aspects of the problem.

The heuristically motivated controller is the simplest. It assumes little knowledge about the controlled system. It is also the structure that offers the weakest theoretical stability results and it has to be tuned more or less by trial and error in order to work. Compared to the other two controllers, it produced reasonable results in the simulations. However, it was not very well suited to handle reference signals with different characteristics. For example, when tuned to achieve good performance for a step of certain amplitude, the controller failed to stabilize the system when exposed to a step of larger amplitude. This is of course a serious drawback, since the objective for the controller was to stabilize the system for all reference signals.

The reference governor was designed to act as a filter for the reference signal. The purpose of the controller was to make sure that certain predefined constraints were not violated. In our case, the control signal saturation constituted the constraint. The task of the reference governor is therefor far more explicit than for the heuristic controller, although they share the same structure. In the simulations, the reference governor performed well, and did indeed stabilize the system for various reference signals. The chattering in the control signal might be a complication. But as shown, it may be cured with a slight degradation of performance.

The last controller to be analyzed was based on a phase plane analysis. While the reference governor explicitly tried to prevent saturation, this controller had no such restrictions. On the contrary, the behavior of the system operating in saturation was studied in detail. This study lead to the cascaded saturations controller. The controller is very aggressive in the sense that it does not prevent saturation. Rather, it uses the saturation limits to push the system towards what is possible, given the constraints. Simulations of this controller showed that it performs very well. It has the best performance of the controllers that have been investigated. A drawback with this method compared to the reference governor is worth mentioning. Whereas the theory of admissible sets is fairly general, the phase plane analysis has to be tailored to each particular system.

To conclude, all three controllers (with some reservations for the heuristic controller) solves the stabilization problem. The two more advanced controllers offer both superior performance and improved stability properties.

An interesting result was that well performing controllers was designed, although the design objectives were very different. The reference governor strive to avoid saturations, whereas the cascaded saturations controller explored the potential of the saturation. An important point to be made, is that the two more advanced controllers uses a considerable amount of knowledge about the plant. This is of course not a problem if the plant and the plant model are similar, but it may become a major complication if this is not the case.

7.2 Experiments

The significance of the results from the analysis of the linearized system proved to be small when applied to the real plant. As discussed, the reference governor and the cascaded saturations controller both assumes much knowledge about the plant. In our case, this proved to be a serious problem. The inherent nonlinearity of the Furuta pendulum, friction and noise are important reasons for this. When applied directly to the real plant, the controllers designed for the linear pendulum model did not work. Some tuning was needed to obtain the desired results. This is, however, to be expected when transferring controllers from a simulation environment to a real plant. Only the heuristic controller and the cascaded saturations controllers were implemented and tested on the real pendulum. Due to extremely poor achievements with filtering and prediction of the pendulum states, the reference governor was not implemented at all.

The rate limiter strategy presented in section 5.1 was easiest to tune and obtain reasonable results with. This method is the simplest of the two tested, in the sense that it assumes little knowledge about the plant. The controller derived from the phase plane analysis in Section 5.3, appeared superior in the simulations, but was more difficult to translate to the real plant. A more thorough tuning process was needed in order to make this strategy work, compared to the rate limiter controller. The phase plane based controller was explicitly designed to push the linear system towards the limit for what was feasible, given the constraints. This fact gives the controller very poor robustness properties, since also small deviations in the real plant compared to the linear model might cause instability.

Having said this, both the controller structures actually solved the problem. The parameters had to be adjusted, but the structures proved to be successfully working.

7.3 Future Work

The controller designs in this work performed very well in simulation. These promising results proved to have little significance on the real pendulum, for reasons discussed above. This suggests several interesting fields for future research.

A first natural extension could be to abandon the linear pendulum model, and work with the nonlinear model instead. This approach would however significantly increase the complexity of the calculations, which is less attractive. This approach is also extremely case specific, in the sense that it translates badly to systems that are not Furuta pendulums.

A more attractive topic would be a robustness analysis. Both the reference

governor and the controller based on the phase plane analysis assumes perfect knowledge about the plant. To explore the consequences of plant uncertainties for these controllers would be an interesting and relevant extension of this work.

8. Implementation

So far all calculations have been done in continues time. The experiments however have been performed using discrete controllers implemented on a computer. This approximation should not affect the validity of the results, since a short sampling period, 10 ms, has been used. Matlab was used for calculations of the discrete controllers.

8.1 Experimental Set Up

A Furuta pendulum, a joystick and a personal computer were used for the experiments. This section describes the set up; connections etc.

The Pendulum The pendulum used for the experiments provides several measured signals; arm position and velocity, pendulum angle and angular velocity. The later signals exist in two separate versions, one that covers all possible pendulum angles and one that only covers angles near the upright position. The top angle measurements were used for stabilization and velocity control, while the the full lap signals were used for the swing up sequence.

The signals from the pendulum were connected to the I/O interface on the computer in the following way:

I/O Connection	*Pendulum Signal*
AI2	Pendulum Angle (Top)
AI3	Pendulum Velocity (Top)
AI4	Arm Position
AI5	Arm Velocity
AI6	Pendulum Angle (360°)
AI7	Pendulum Velocity (360°)
AO0	Control signal
Ground	Ground

The Joystick A joystick connected to the computer offers a quite good reference generator when to demonstrate manual control, but for the experiments computer generated reference signals were used in order to enable fair comparison between the different strategies. The joystick signal (only the X axis signal was used) represents the desired velocity of the pivot point. For power supply a DC servo were used. Connections were made as follows:

I/O Connection	*Joystick Signal*
AI0	White (X Axis)
AI1	Blue (Y Axis)
DC Servo, +9V	Red
DC Servo, Ground	Black

The Computer A PC, 450 MHz Pentium II, running Linux as operating system and an I/O interface connected to it was used. For all simulations and experiments Matlab 5.3 in combination with Simulink was used.

8.2 The Simulink Interface

All control structures has been calculated using Matlab and implemented in Simulink. Simulink in combination with the I/O interface (see Andersson and Blomdell (1991) offers the possibility to easily evaluate controllers by simulation before performing the experiment on the real pendulum.

A few practical advises are worth mentioning to ease the procedure of reconnecting the pendulum reproducing a well functioning demonstration.

Firstly, it is critical to make sure that the measured signals are transformed from Volts to rad, rad/s etc in a proper way. This is done by examining the signals in the block *Process/Hardware/Conversion of Inputs*. Especially it is critical to make sure that the measurements of the θ angle is zero when the pendulum is in upright position.

Further it is possible that the tracking coefficients has to be adjusted, in order to achieve accurate static reference following. This is done by modifying the blocks *Controller / Reference/Conroller/Johan Heuristic/Tracking* and *Controller / Reference/Conroller/Double Loop/Tracking* respectively.

8.3 Problems Experienced

In this section some of the practical problems experienced during the project will be discussed.

A major problem at the beginning of the project was measurement noise. Although stabilization of the pendulum was possible, it was hard to distinguish the signals, (this problem was most serious for the angular velocity of the pendulum) because of noise. The most significant reason for this was that the pendulum and the computer were connected to power supplies with common ground point far from the plugs. This caused a long ground loop which received a lot of noise. The problem was significantly reduced when pendulum and computer were connected to plugs close to each other. Shielded cables were used for the measured signal with the most severe noise and the control signal. This reduced the noise further. The remaining noise was found to be acceptable.

A problem that appeared right after the swing up sequence finished was a high frequent oscillation in the pendulum. High frequent is here meant to be compared to the natural frequency of the pendulum. Since the frequency of this oscillation was higher than the bandwidth of the closed loop system it could not be damped by the control law. Our solution to the problem was to simply damp the oscillation manually.

A problem experienced in Simulink is worth to mention. The original idea was to include both a model of the pendulum and the hardware interface in the same structure, enabling fast and easy switching between simulation and experiment. However, this turned out to be a problem since the continuous states of the model required to much calculation time when experiment were performed on the real pendulum. It was not possible to keep up the sampling rate which was unacceptable. The solution was to remove the pendulum model during the experiments and insert it for the simulations.

A phenomena that grew more and more significant during the project were periodic spikes in the “jitter” curve. The measured signals exabited more

or less significant discontinuities at those times. This problem caused a lot of confusion, but was tracked down to depend on the numerous Scopes used in the application for debugging purposes. When the Scope buffers were updated every fifth second, the sampling time could not be held. The problem was solved by removing the scopes from the application.

Appendix

A. LQ Summary

The topic of Linear Quadratic optimal control is well documented in the literature (see for example (Åström and Wittenmark (1997), Bitmead *et al.* (1990)). A brief summary of the technique and its basic properties is given here, which should be enough to follow the calculations in the text. Further information can be found in the references.

The foundation upon which the LQ-theory relies is the quadratic cost function, which may be written:

$$\begin{aligned} J &= \int_0^\infty x^T Q x + u^T R u dt \\ Q &\geq 0 \\ R &> 0 \end{aligned}$$

for the continuous time case with infinite time horizon. The objective is defined as designing the (state feedback) controller that minimizes this criterion. The design variables that determines the performance of the resulting controller are Q and R, which both have intuitive interpretations. Q is used to allocate penalty weights to the states, while R is used to penalize the control signal.

The assumption on the controller structure is that all states are available (either through direct measurement, or through estimation (LQG)) for state feedback:

$$u = -Lx$$

Under these assumptions the solution is given by:

$$L = R^{-1} B^T S$$

where S satisfies the Algebraic Riccati Equation (ARE):

$$A^T S + SA - SBR^{-1} B^T S + Q = 0$$

The LQ controller has several useful properties, of which its stabilizing ability is the most important.

The matrix S may be used to form a Lyapunov function:

$$V(x) = x^T S x$$

Lyapunov theory specifies three condition for Lyapunov stability:

1. $V(x) = 0, \quad x = 0$
2. $V(x) > 0, \quad x \neq 0$
3. $\dot{V}(x) \leq 0$

It is obvious that the first condition is satisfied. The second is satisfied since S is positive definite. To show the third, let us rearrange at the ARE

given above.

$$\begin{aligned} A^T S + SA - SBR^{-1}B^T S + Q &= 0 \\ A^T S + SA - SBR^{-1}B^T S + SBR^{-1}B^T S - SBR^{-1}B^T S + Q &= 0 \\ (A - BR^{-1}B^T S)^T S + S(A - BR^{-1}B^T S)^T + SBR^{-1}B^T S + Q &= 0 \\ A_{cl}^T S + SA_{cl} + \bar{Q} &= 0 \end{aligned}$$

The last equation may be recognized as a Lyapunov equation for the closed loop system with system matrix A_{cl}.

Now, calculate the time derivative of the proposed Lyapunov function

$$\dot{V}(x) = x^T \dot{S} x + \dot{x}^T S x + x^T S \dot{x}$$

Using that $\dot{S} = 0$ (steady state condition) and $\dot{x} = A_{cl}x$ the Lyapunov stability condition becomes

$$\dot{V}(x = x^T (A_{cl}^T S + SA_{cl})x = -x^T \bar{Q} x \leq 0$$

which is clearly fulfilled since $\bar{Q}$ is (at least) positive semidefinite.

These calculations are valid for a linear system. When the controller based upon a linearized model of the true plant, which is most likely different from the linearized model, the stability result might have limited validity.

B. Admissible Set Theory

In this section, an overview of admissible set theory will be given. In addition an application of admissible sets, the reference governor will be discussed. For a more complete description, see Gilbert and Tan (1991) and Gilbert *et al.* (1994).

B.1 Admissible Sets

Stability can always be achieved when a controllable linear system is controlled by state feedback. That is, given any state configuration, the controller will recover the system to its equilibrium. When nonlinearities are introduced in the feed back loop, global stability is no longer guaranteed. In this case there might exist some state configuration for which the controller can recover the system, and some for which it cannot. This reasoning leads us to the notion of admissible and non admissible sets.

In this section we will use a discrete time formulation of the problem. Assume a state feedback controlled linear system

$$\begin{aligned} x_{k+1} &= A_p x_k + B_p u_k \\ u_k &= L x_k \end{aligned} \tag{15}$$

yielding the closed loop system

$$x_{k+1} = A x_k = (A_p + B_p L) x_k.$$

which is assumed to be asymptotically stable. Further, assume that the system 15 is subject to constraints. By choosing a matrix C and a set Y we can express a wide range of constraints by set inclusion

$$y_k = C x_k \in Y.$$

We shall in the following assume that Y may be written as

$$Y = \{y : f_i(y) \leq 0,\ i = 1, \cdots, s\}$$

We may now restate the problem,

$$\begin{aligned} x_{k+1} &= A x_k \\ y_k &= C x_k \end{aligned} \tag{16}$$

subject to the constraints

$$y_k \in Y,\ k \geq 0.$$

This formulation is quite general and may be used to express various constraints, involving the state variables. Assume, for example, a control signal saturation, $|u| \leq u_{sat}$. We may then choose $y_k = u_k$, yielding $C = L$, and $Y = [-u_{sat}, u_{sat}]$.

A method for determining a maximal admissible set for the constrained system (16) is presented in Gilbert and Tan (1991). In this work, the maximal admissible set is defined as

$$O_\infty(A, C, Y) = \{x : C A^k x \in Y,\ k \geq 0\}. \tag{17}$$

This definition can be interpreted as follows. If an initial condition is chosen so that $x_0 \in O_\infty$, then the resulting state trajectories will not leave O_∞. Also, the state trajectories will not violate the constraints.

It now remains to calculate O_∞. The definition (17) can be restated as

$$O_\infty = \{x : f_i(CA^k x) \leq 0,\ i = 1, \cdots, s,\ k \geq 0\} \tag{18}$$

which may be used to calculate O_∞. The problem is then that we will obtain an infinite number of inequalities restricting x as $k \to \infty$. To solve this problem Gilbert and Tan (1991) suggests the following algorithm.

1. Set $t = 0$.
2. Solve the following optimization problems for $i = 1, \cdots, s$:

   $$\text{maximize } J_i = f_i(CA^{t+1}x)$$

   subject to the constraints

   $$f_j(CA^k x) \leq 0,\ j = 1, \cdots, s,\ k = 0, \cdots, t.$$

   Let J_i^* be the maximum value of $J_i(x)$. If $J_i^* \leq 0$ for $i = 1, \cdots, s$, stop. Set $t^* = t$ and define O_∞ by

   $$O_\infty = \{x : f_i(CA^k x) \leq 0,\ i = 1, \cdots, s,\ k = 0, \cdots, t^*\}$$

   Otherwise continue.
3. Replace t by $t + 1$ and return to step 2.

The complexity of this algorithm dependents very much on the constraint functions $f_i,\ i = 1, \cdots, s$. However, if these functions are linear, The algorithm becomes quite simple, however, if these functions are linear. The optimization problem may then be solved by linear programming, and explicit solutions for the inequalities are available.

The results given in this section are brief. For a thorough discussion about admissible sets, see Gilbert and Tan (1991). Extensions and simplifications are given in McNamee and Pachter (1998).

B.2 The Reference Governor

An interesting application of admissible sets is the reference governor presented in Gilbert *et al.* (1994). The idea is to use a precalculated admissible set for a given system, to design a controller that guarantees stability independently of the reference signal. The aim of the reference governor is to ensure that the system never undertakes a state where the given constraints are violated, i.e. $x \in O_\infty,\ k \geq 0$.

Consider the system

$$\begin{aligned} x_{k+1} &= Ax_k + Bw_k \\ u_k &= Cx_k + Dw_k \ \in \ Y \end{aligned} \tag{19}$$

This system is equivalent to (16) but it is extended to also take the reference signal w_k into account. As before, the matrix A is assumed to have its characteristic roots inside the the unit circle. The mission of the reference governor, is to generate w_k from r_k. Gilbert *et al.* (1994) suggest the following algorithm

$$w_{k+1} = w_k + K(r_k, x_k^G)(r_k - w_k),\ x_k^G = \begin{pmatrix} w_k \\ x_k \end{pmatrix},\ K(r_k, x_k^G) \in [0,1].$$

The signal r_k is thus low pass filtered before it is fed into the system. The critical feature of the reference governor is the variable gain $K(r_k, x_k^G)$. K is used to adjust the bandwidth of the filter, dependent on the state of the system and the reference signal. If K is equal to one, the only effect of the reference governor is that the reference signal is delayed one sampling interval. For smaller values of K, the filtering of r_k becomes significant.

Let us rewrite the system 19 to also include the reference governor

$$\begin{aligned} x_{k+1}^G &= A_G x_k^G + B_G K(r_k, x_k^G)(r_k - (I\ 0)x_k^G) \\ y_k &= C_G x_k^G \ \in Y \\ A_G &= \begin{pmatrix} I & 0 \\ B & A \end{pmatrix},\ B_G = \begin{pmatrix} I \\ 0 \end{pmatrix},\ C_G = (D\ C). \end{aligned} \tag{20}$$

Now, it is necessary to guarantee that $y_k \in Y$ at all times. A reasonable strategy is to ensure that no constraints are violated if $K(r_\tau, x_\tau^G) = 0,\ \tau \geq k$, for some k. This objective is achieved if at every sample, $K(r_k, x_k^G)$ is chosen so that $x_{k+1}^G \in O_\infty(A_G, C_G, Y)$. This means that $K(r_k, x_k^G)$ has to be chosen as

$$K(r_k, x_k^G) = \max\{\alpha \in [0,1] : A_G x_k^G + B_G \alpha(r_k - (I\ 0)x_k^G) \in O_\infty(A_G, C_G, Y)\}$$

Before we proceed, let us consider the equilibria which may be achieved by the reference governor. In steady state, we have $x_{k+1} = x_k$ and for the system (19) this gives

$$\begin{aligned} W_0 &= \{w : H_0 w \in Y\} \\ H_0 &= D + C(I - A)^{-1}B. \end{aligned}$$

Since $w_k = r_k$ in steady state, we get the additional condition $r_k \in W_0$. This gives us the expressions needed to evaluate $K(r_k, x_k^G)$

$$\begin{aligned} \alpha_{ij} &= \max\{\alpha \in [0,1] : f_i(C_G A_G^j(A_G x_k^G + B_G \alpha(r_k - (I\ 0)x_k^G))) \leq 0\} \\ \alpha_i &= \max\{\alpha \in [0,1] : f_i((H_0\ 0)(A_G x_k^G + B_G \alpha(r_k - (I\ 0)x_k^G))) \leq 0\} \\ K(r_k, x_k^G) &= \min\{\alpha_{ij} : i = 1, \cdots, s,\ j = 0, \cdots, t^*\} \cup \{\alpha_i : i = 1, \cdots, s\} \end{aligned}$$

In principle, it is now possible to proceed and implement the reference governor. However, some practical considerations are worth mentioning. The calculation of $K(r_k, x_k^G)$ has to be performed within one sampling interval. This implies that the expressions for evaluation of K given above might

not be very well suited for implementation. (For simulation purposes they should be sufficient however.) Gilbert *et al.* (1994) and also McNamee and Pachter (1998) give several suggestions for simplifying the description of O_∞, by calculating an approximate version, O_∞^ε of the admissible set. Typically the methods strives to reduce the number of inequalities needed to define O_∞. Fewer inequalities to evaluate yields a less complex computation of K, and shorter calculation time.

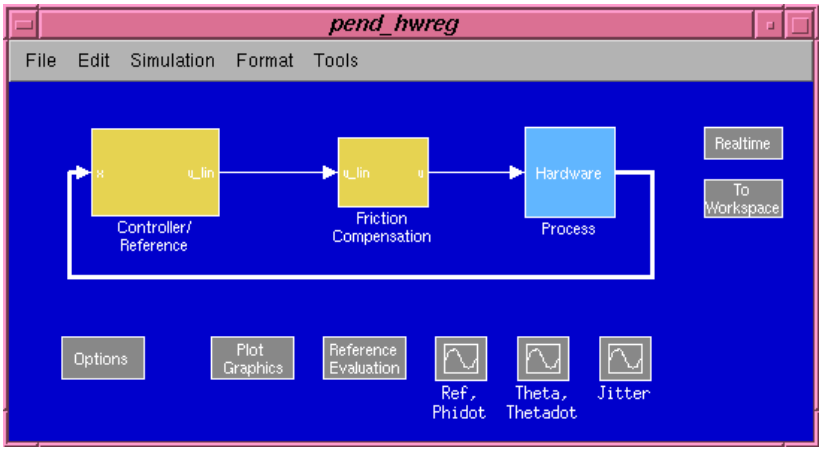

Figure 27 The main view of the user interface.

C. User Interface

The main view of the user interface is seen in fig 27. All relevant plots and controls should be located in this view. To start the demonstration, make sure the pendulum is at rest (either hanging down or standing upright) and press *Ctrl+t*. If the pendulum was at rest hanging down, the swing up sequence is started by moving the joystick in any direction along the x-axis. When the pendulum has reached its upright position the velocity of the pendulum can be controlled.

A few buttons appear in the main view, their function is explained by the following table: Both control of the real pendulum and simulation using a model is possible. However the pendulum model is not included when control of the real pendulum is performed. If it was, the sampling rate may not be kept since the continuous states of the model takes too much calculation time. Instead the model has to be imported before simulations can be done. The model is stored in the file *pend_model.mdl* and should be imported to the block *Process*. Double click the block *Process* to enable the simulation.

Button	*Function*
Options	The application may be set to operate in two modes, either open loop or closed loop. Closed loop is normally used, but open loop may be used for debug purposes. In the later case no control signal is given to the process, but all measured signals are logged. Further, two ways of generating reference the signal is allowed. Either the joystick or a sequence of reference steps. It is possible to change the step sequence by modifying the block *Controller/Reference* / *Controller* / *Reference generator*. Finally, any of the implemented strategies may be selected.
Plot Graphics	Displays a plot showing θ, $\dot{\theta}$, φ, $\dot{\varphi}$, u and jitter
Reference Evaluation	Displays the loss function as well as the reference signal and response. Also calculates rise times. (Works best when the step sequence is used.)
Ref, $\dot{\varphi}$	A real time plot showing the reference and phidot.
θ, $\dot{\theta}$	A real time plot showing θ and $\dot{\theta}$.
Jitter	A real time plot of the jitter.

D. References

Andersson, L. and A. Blomdell (1991): "A real-time programming environment and a real-time kernel." In Asplund, Ed., *National Swedish Symposium on Real-Time Systems*, Technical Report No 30 1991-06-21. Dept. of Computer Systems, Uppsala University, Uppsala, Sweden.

Åström, K. J. (1999): "Limitations on control system performance.". Department of Automatic Control, Lund Institute of Technology.

Åström, K. J. and K. Furuta (1999): "Swinging up a pendulum by energy control." *Automatica*. To be published.

Åström, K. J. and B. Wittenmark (1997): *Computer-Controlled Systems*, third edition. Prentice Hall.

Bitmead, R. R., M. Gevers, and V. Wertz (1990): *Adaptive Optimal Control, The Thinking Man's GPC*. Prentice-Hall, Englewood Cliffs, New Jersey.

Brufani, S. (1997): "Manual control of unstable systems." Master thesis ISRN LUTFD2/TFRT--5576--SE. Department of Automatic Control, Lund Institute of Technology, Lund, Sweden.

Burg, T., D. Dawson, C. Rahn, and W. Rhodes (1996): "Nonlinear control of an overhead crane via the saturating control approach." In *Proc. of the 1996 IEEE International Conference on Robotics and Automation*, pp. 3155–3160. Minneapolis, Minnesota.

Canudas de Vit, C., K. J. Åström, and K. Braun (1987): "Adaptive friction compensation in DC-motor drives." *IEEE Trans. Robotics and Automation*, **RA-3**, pp. 681–685.

Eker, J. and K. J. Åström (1996): "A nonlinear observer for the inverted pendulum." In *Proc. IEEE Conference on Control Applications*, pp. 332–337. Dearborn, Michigan.

Gäfvert, M. (1998): "Derivation of furuta pendulum dynamics." Technical Report. Department of Automatic Control, Lund Institute of Technology, Lund, Sweden.

Gilbert, E., I. Kolmanovsky, and K. Tan (1994): "Nonlinear control of discrete-time linear systems with state and control constraints: A reference govenor with global convergence properties." In *Proc. 33rd Conference on Decision and Control*, pp. 144–149. Lake Buena Vista, Florida.

Gilbert, E. and K. Tan (1991): "Linear systems with state and control constraints: The theory and application of maximal output admissible sets." *IEEE Trans. on Automatic Control*, **36:9**, pp. 1008–1020.

McNamee, J. and M. Pachter (1998): "The construction of the set of stable states for constrained systems with open-loop unstable plants." In *Proc. of the American Control Conference*, pp. 3364–3368. Philadelphia, Pennsylvania.

Olsson, H. (1996): *Control Systems with Friction*. PhD thesis ISRN LUTFD2/TFRT--1045--SE, Department of Automatic Control, Lund Institute of Technology, Lund, Sweden.

Patcher, M. and R. Miller (1998): "Manual flight control with saturating actuators." *IEEE Control Systems*, February, pp. pp. 10–19.

Rundqwist, L., K. Stål-Gunnarsson, and J. Enhagen (1997): "Rate limiters with phase compensation in jas 39 gripen." In *Proc. European Control Conference*. Saab Military Aircraft, Linköping, Sweden.

Stein, G. (1990): "Respect the unstable." Bode Lecture.

Åström, K. and S. Brufani (1997): "Manual control of an unstable system with a saturating actuator." In *Proc. 36th Conference on Decision and Control*, pp. 964–965. San Diego, California.

Svensson, J. (1998): "Effects of friction on the Furuta pendulum." Master thesis ISRN LUTFD2/TFRT--5593--SE. Department of Automatic Control, Lund Institute of Technology, Lund, Sweden.